AMERICAN UNIVERSITY OF BEIRUT

LIGHTNING SCRAMJET INTERACTION THEORETICAL AND NUMERICAL INVESTIGATION

by
NIDAL JAMAL FARRAN

A thesis
submitted in partial fulfillment of the requirements
for the degree of Master of Engineering
to the Department of Mechanical Engineering
of the Maroun Semaan Faculty of Engineering and Architecture
at the American University of Beirut

Beirut, Lebanon
April 2019

AMERICAN UNIVERSITY OF BEIRUT

LIGHTNING-SCRAMJET INTERACTION THEORETICAL INVESTIGATION.

by

NIDAL JAMAL FARRAN

Approved by:

Dr. Fadl Moukalled, Professor
Mechanical Engineering
Advisor

Dr. Nesrine Ghaddar, Professor
Mechanical Engineering
Member of Committee

Dr. Kamel Abu Ghali, Chairperson and Professor
Mechanical Engineering
Member of Committee

Date of thesis defense: April 24rth, 2019

AMERICAN UNIVERSITY OF BEIRUT

THESIS, DISSERTATION, PROJECT RELEASE FORM

Student Name: ____Farran_____Nidal _____Jamal _____
Last First Middle

● Master's Thesis ○ Master's Project ○ Doctoral Dissertation

☐ I authorize the American University of Beirut to: (a) reproduce hard or electronic copies of my thesis, dissertation, or project; (b) include such copies in the archives and digital repositories of the University; and (c) make freely available such copies to third parties for research or educational purposes.

☒ I authorize the American University of Beirut, to: (a) reproduce hard or electronic copies of it; (b) include such copies in the archives and digital repositories of the University; and (c) make freely available such copies to third parties for research or educational purposes
after:

One ---- year from the date of submission of my thesis, dissertation, or project.

Two ---- years from the date of submission of my thesis, dissertation, or project.

Three ● years from the date of submission of my thesis, dissertation, or project.

[signature] 2nd May, 2019

Signature Date

ACKNOWLEDGMENTS

First of all, I would like to express my very profound gratitude to my Beloved Mother and my Father in the Heaven for believing in me and always supporting me to reach a high educational level.

Special thanks to my thesis' advisor, Professor. Fadl Moukalled for adopting my Thesis' Idea and paving the way to achieve my dream in the Aerospace Field.

I would also like to thank my committee members, Professor. Nesrine Ghaddar and Professor. Kamel Abu Ghali for their significant remarks and their encouraging words.

AN ABSTRACT OF THE THESIS OF

Nidal Jamal Farran for Master of Engineering
Major: Mechanical Engineering

Title: Lightning Scramjet Interaction Theoretical and numerical Investigation

Based on the literature regarding the scramjets and the plasma aerodynamics field in the hypersonic or supersonic flow, plasma actuators or spark discharge devices are used to control the shockwave-boundary layer interaction characteristics occurring in a scramjet for supersonic flows where the resulted separated zone could be enlarged due to the plasma actuator as well as the shockwaves structures induced by the wedge or ramp angle could be varied.

As a matter of fact, all of these modified supersonic characteristics are induced by a Micro-Electro-Mechanical Systems (MEMS) device which is made by humans, that means it was about an artificial arc discharge which leads to new compressible phenomena.

Therefore, this kind of plasma aerodynamics research pushes me up to wonder what will happen if a natural arc discharge strikes a scramjet flying in a supersonic flow knowing that the natural lightning phenomenon and the artificial spark discharge are not similar where they have different parameters such as the temperature, the generated heat and there are so many parameters in the process of investigation.

Lightning discharge is simulated using ANSYS FLUENT where the Magneto hydrodynamics equations and terms are adopted and coupled with the Navier Stokes equations to be applied and executed along with the phenomenon of a supersonic flow over a scramjet inlet's compression corner.

In other words, the interaction between the lightning discharge and the shockwave generated by the ramp or the compression corner are simulated leading to novel results which are not discovered before. Within a time interval of nearly 1 ms, the shockwave wave structure will be modified by the propagating intense lightning strike.

On the other hand, a second gap is discovered where analytical or theoretical formulae regarding the propagation of a blast wave in a compressed medium were not found. In fact, this phenomenon was just done experimentally as well as numerically.

Static Pressure, Static Temperature and the density's analytical solution were developed to fill in the literature's gap using the Rankine-Hugoniot jumping relations.

CONTENTS

ILLUSTRATIONS

CHAPTER 1

INTRODUCTION

1.1. Historical Background

1.1.1. Physics of Lightning

Lightning is a natural phenomenon where it was taking place before the human race creation on our planet. In fact, lightning is regarded as a powerful electrical discharge in air having a high current intensity where this long arc discharge‘s length is expressed in miles whereas the width or the diameter should be about one or two inches. Usually, the maximum lightning current could be more than 10000 A and a temperature of nearly 28 000 °C which is 5 times hotter than the sun‘s surface temperature where for this high temperature, the gas will be ionized and thus it will be regarded in a plasma state having positively and negatively charged ions.

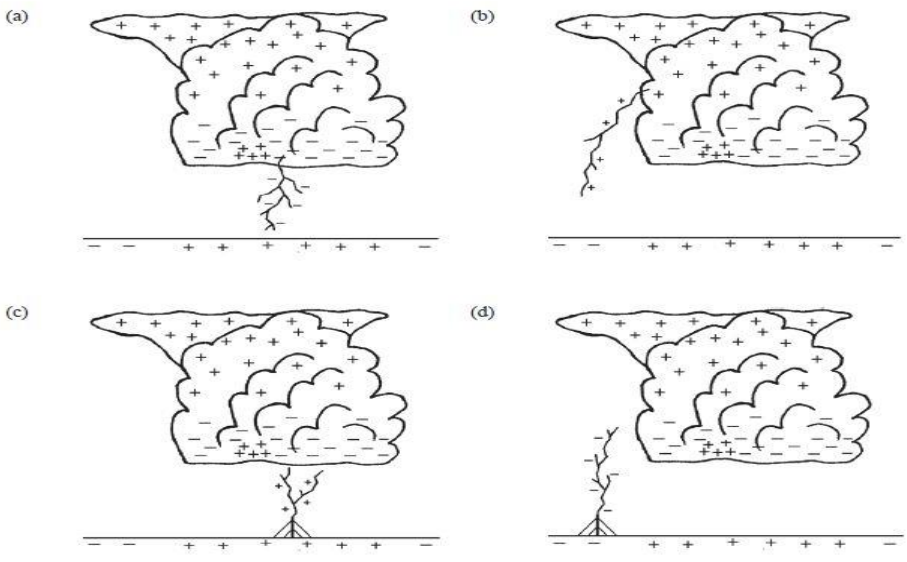

FIG.1. Cloud to ground lightning discharge main types. (SOURCE: *Nature of Atmospheric Discharges)*

According to Carol[1] there are four main types of atmospheric phenomenal air discharges. Lightning could occur starting from the cloud toward the ground (cloud to ground lighting “CG”), as well as it could be within the cloud (Intra-Cloud lightning “IC”), Inter-Cloud lightning “CC” which takes place between clouds and finally the cloud to air lightning “CA”. The most frequent lightning type is the Intra-Cloud and the Cloud to ground discharges, where the latter could be in four principal forms as such in the figure below.

In the sub-figure 1a) we have a negatively descending cg type whereas 1b) represents the positively descending cg. on the other hand, the positively ascending cg type is shown in 1c) and 1d) exhibit the negatively ascending one.

where Fig.1 represents the first phase of each CG type, knowing that 1a) is the most common CG phenomenon so let us describe the subsequent phase of the negatively descending CG lightning discharge starting from 1a), the leader of the lightning current moves downward oriented to the ground direction through steps where the latter are sub-divided into many branches moving in several directions where the average leader current could be ranging from 100 A to 1000 A .

As the leader moves downward, the electrical field will be increased so in case there is a sharp object placed on the ground hence the resulted huge potential will create streamers ten meters above closing the lightning current channel as shown in Figure 2b).

In fact, the flash that we usually observe during the lightning procedure is a series of approximately five strokes where the period between each stroke could be about 10 ms. Moreover, each stroke moving from the cloud to the ground consists of a leader navigating downward plus a subsequent return stroke traveling upward taking the

leader's path as shown in figure 2c) where the role of the return stroke is distributing positive charges in order to make a neutralization with the negative charges emitted by the leader. Among the series, the highest peak current having a potential difference between the ground and the cloud generates a sudden huge energy that heats the long arc charge to a temperature greater then 30 000 °C leading to a pressure rise equal and greater than 10 times of the atmospheric pressure therefore a shockwave will be produced and obviously this is the intense sound wave called "thunder" which we usually hear. In case we have an excess of charges inside the cloud, a stream called "dart leader" could propagate downward through the lightning channel after the return stroke upward movement creating a subsequent return stroke represented in Figure 2d).

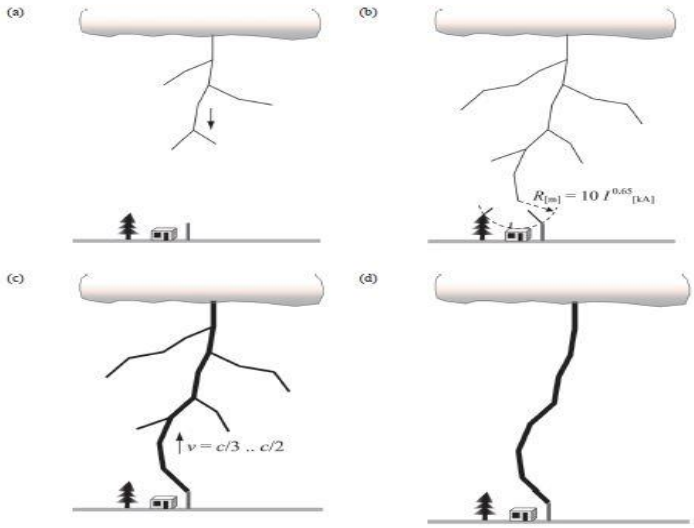

FIG.2. Cloud to ground lightning discharge type mechanism (SOURCE: *Nature of Atmospheric Discharges)*

1.1.2 Magneto-hydrodynamics and Plasma Overview.

Let's begin with Plasmas where it is firstly named in the field of Medicine Sciences by a Czech scientist. In fact, our blood system contains a transparent liquid

holding proteins and cells and characterized by a high viscosity. In the middle of the nineteenth century Johannes Purkinje gives this liquid the name Plasma, an old Greek work, which means a viscous fluid that didn't flow easily. In 1927, the American chemist Irving Langmuir has made the analogy between the red and white corpuscles that is contained by the plasma blood and the electrons and the protons (ions) that are carried by the ionized high temperature fluid, hence the fourth state of matter's name as known as Plasma.

When a gas is subjected to a high temperature, the excess of thermal energy ionizes the atoms leading to free moving electrons where the concentrations of the positive and negative charges are equal so that in most of the cases, the plasma is regarded as a neutral state. However, the because of the existence of moving charges and ions, the interaction between electric and magnetic fields along with the plasma is possible.As a matter of fact, a neutral gas could be differed by a plasma where the inter-atomic or inter-molecular forces in neutral gas are powerful and more important in short distances. On the other hand, the kind of the forces between particles is electromagnetic where the fact that the particles are charged, so that each particle exerts coulomb forces on another one. Moreover, a moving charge produces a magnetic field leading to the creation of the Lorentz force on another charged particle. Figure 3 provides a concept in order to distinguish a neutral gas to a plasma where the image in the left hand side presents the atoms in a neutral gas whereas those of the plasma are shown in the right hand side image.

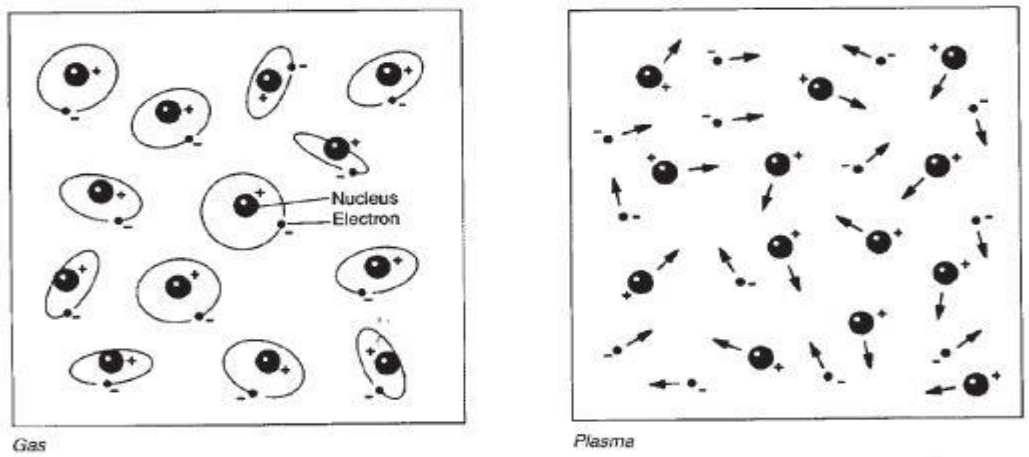

FIG.3. Difference between Neutral Gas Particles and Plasma Particles. (SOURCE: *Goossens, M. (2003). An Introduction to Plasma Astrophysics and Magnetohydrodynamics. Dordrecht: Springer Netherlands.)*

The Beginning of the evolution of plasma sciences is triggered through the discovery of Plasma Sheath phenomenon by Langmuir. When the Plasma is connected to a wall, free electrons are moving with a high kinetic energy due to their extremely hot temperature as well as their mass is too small compared to that of the ions. Therefore this fact leads to a un-equilibrium between the fluxes between the two opposite charged particles which induce a negatively charged wall surface where the latter repels incoming electrons into the plasma and then the concentration of electrons decreases with respect to positive as well as neutral particle forming a layer called plasma sheath. On the other hand, several scientists strived to develop theories about the propagation of electro-magnetic waves in a non uniform magnetized plasma where these theories are helpful to solve radio communication problems such as the distortion of radio waves in the ionosphere.

Furthermore, plasmas are emphasized in several astrophysical phenomenon investigations so in order to deal with these kinds of problems in a sophisticated manner, the Swedish plasma physicist and electrical engineer Hannes Alfvén used to be the first scientist to initiate the magneto-hydrodynamics theories adopting plasma as a

conducting fluid in 1940, where MHD applications will be discussed in the next sub section.

In 1958, scientists focus the attention on the plasma thermonuclear fusion research investigation. Typically, a gas containing the two Hydrogen isotopes such as Deutrium"^{2}H" and Tritium "^{3}H" is subjected to a high temperature in order to acquire a powerful kinetic energy making the repulsion force between the particles to be negligible so that the latter will be able get closer and to fuse. At a critical temperature, nearly 10^{8} K, the Hydrogen isotope particles becomes ionized where free electrons are about to leave their atoms and the latter turn out to be ions or positive charges leading to the formation of the plasma, the fourth state of matter. Due to the huge temperature, the plasma particles are so agitated that it moves back and forth in a fast manner where there will be a high probability for the contact between plasma charges and the wall surface leading to several kinds of dangerous damage, in addition to the failure of the desired research objectives where the plasma get cooler. So to prevent all of the mentioned problems, scientists has adopted the Magneto-hydrodynamics theories knowing that the plasma carries ions and negatively moving charged particles so that it is feasible to apply a magnetic field in order to avoid the chaos and to maximize the organization of the charged particles paths into a specified and restricted zone known as the magnetic confinement. In fact, scientist has invented a material which as a toroïdal form to confine the plasma, the most famous magnetic confinement equipment is the Tokamak.

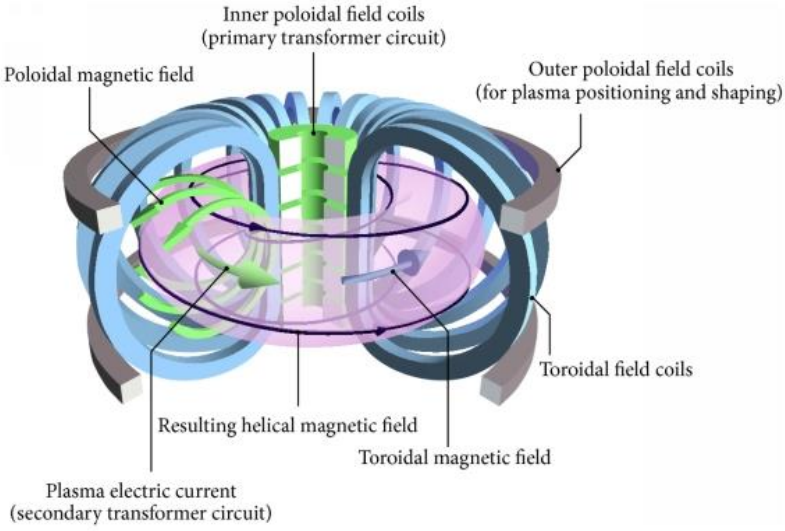

FIG.4. Magnetic confinement (SOURCE : S. LI, H. JIANG, Z. REN, C. XU - S. LI ET. AL. "optimal tracking for a divergent-type parabolic pde system in current profile control")

The Figure above provides a quick glace for what is recently discussed about the magnetic confinement of the thermonuclear plasma inside the Tokamak. In addition to the aforementioned applications, there are other natural plasmatic phenomena specifically in the upper atmosphere as well as the ionosphere and above. The most common and interesting topic in astrophysics throughout the history is the Sun where there are several points to be investigated. In fact, the solar corona which is defined as the external atmospheric layer of sun, is extremely hot so that it dilates supersonically leading to the generation of electrons and protons in a way to satisfy the main characteristics responsible for a creation of a plasma where the existence of a small concentration of other ionic particles is available but could be neglected in some applications. The solar wind could reach the orbit of the earth with a velocity of more than a thousand times of the sound speed (340 m/s) as well as a temperature of nearly 10000 K.

The figure below is discovered and taken from NASA shows the solar corona sighted through the solar eclipse where the moon coincides with the locus of the sun and prevents the sun rays to be observable through the naked eyes leaving the surrounding shining light.

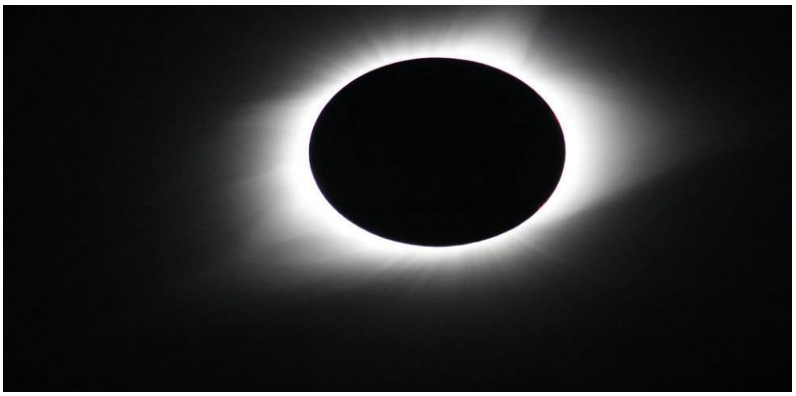

FIG.5. solar corona (source : nasa's goddard space flight center/gopalswamy)

The solar wind bombarded from the sun holds the Interplanetary Magnetic Field "IMF" with it while traveling between planets where the high speed flowing plasma's magnetic field has been raised due to the solar magnetic activities. The magnetosphere, the region where the magnetic field generated by the earth is a supreme one which is able to magnetically control the neighboring particles, is mainly compressed through the part facing the sun by the supersonic solar wind powerful pressure leading to a parabolic structure until it reaches the equilibrium between the pressure of the incoming plasmatic beam and earth's magnetic pressure to produce the external layer of the magnetosphere called the magnetopause. A bow shock will be appeared, when the solar wind incrusts the magnetosphere with a velocity of 0.0013 times the light celerity.

Since there is a part of the solar wind is propagating along the whole earth and its magnetic system, the part of the earth magnetism, which is not totally covered by

the sun rays so that it is not directly bombarded by the solar particles, gets extended to a large distance forming the magnetotail. Figure.7 represents the scheme of the solar wind-earth magnetism interaction.

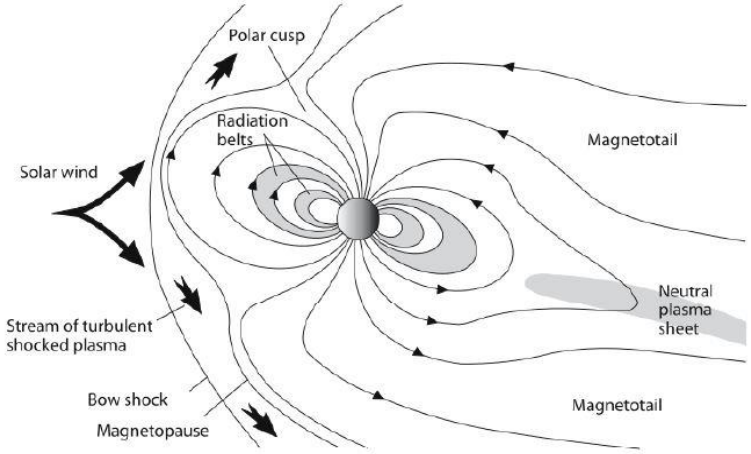

FIG.6. Magnetosphere of the Earth Planet (source : Lanza, R. and Meloni, A. The Earth's Magnetism – An Introduction for Geologists.Würzburg: Springer, 2006.)

Despite the fact that the magnetosphere's boundary layer is resistant to solar wind particles to break through, a small portion of positive ions and electrons has been leaked into the magnetosphere's interior system where these charged particles are affected by the earth magnetic field's Lorentz force inducing the spiral-transitional movement around and along with the magnetic field lines surrounding the earth planet. When the spiraling movement of the particles reach the poles where the magnetic field lines are narrower more concentrated and more powerful, the particles are subjected to a repulsion into the other hemisphere and the same procedure will be taking place leading to an alternative movement between the poles and the hemispheres generating the Radiation Belts. There is another part of electrons left where they possess a huge level energy to infiltrate the upper atmosphere and to impact with the existing atoms leading

to a variation of the collided particles energy states where this gradient triggers the emittance of electromagnetic packet of photons through the earth's poles that assemble to form visible lights to humans called Auroras.

The figure below shows the Aurora Australis which appeared in the Earth's southern pole and taken from a NASA space shuttle.

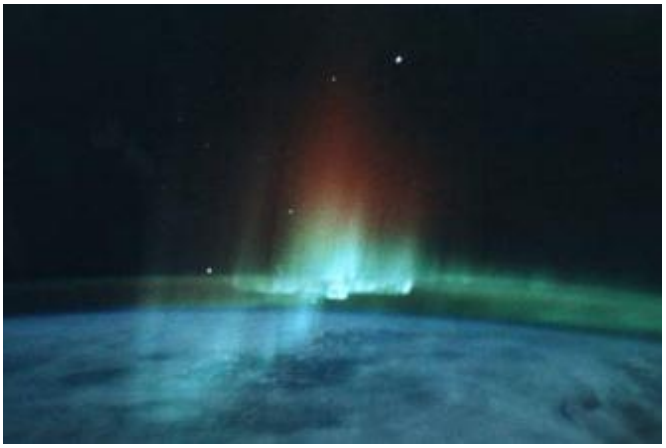

FIG.7. AURORA AUSTRALIS (SOURCE : NASA.)

The final brief description I want to make is to give a quick review about Lightning Plasma physics. As a matter of fact, the physics of lightning could be categorized in the field of Space Plasmas since a sudden high temperature in the range of 25000K ionizes the atmosphere turning it into the fourth state of matter. When modeling lightning discharge, scientists focus not only on the tremendous temperature but also on the massive pressure resulted from the intensive current as well as on the magneto-hydrodynamics effects leading to the three main widespread methods…

The first one is based on the famous fluid dynamics theories, the Navier-Stokes equations along with the magneto-hydrodynamics magnetic induction equation in order to model the space plasma physics of lightning; this is known by the macroscopic method. On the other hand, Boltzmann and Maxwell equations are adopted to solve the

mid-scale between macroscopic and microscopic scales problems which is the mesoscopic method. Finally, the fundamentals of the statistical physics field such as the dynamics of single charged theory along with the perturbation theory are required to deal with microscopic approximations of the problem where macro parameters and variables are determined using particle probability functions calculations. “Particle in Cell” numerical method is the most suitable strategy to model microscopic phenomena and applications. In the current thesis, lightning modeling will be spotted in the following chapters where the magneto-hydrodynamics equations will be performed to deal with the desired thesis objectives. Figure.8, represents all of the nature phenomena and applications which belongs to the plasma state category and placed in terms to the variations of temperature with respect to the number of particles density.

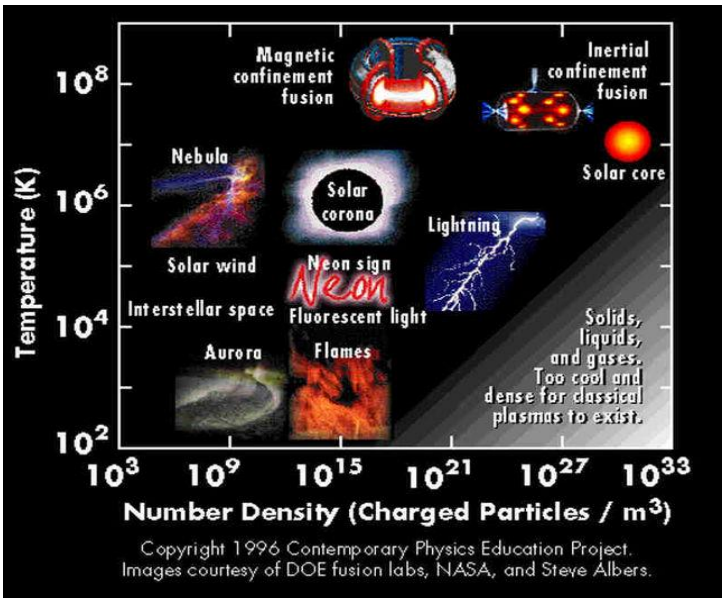

FIG.8. Plasma Categories (source : Copyright [www.cpepweb.org Contemporary Physics Education Project].Images courtesy of DOE fusion labs, NASAm and Steve Albers.)

1.1.3 Air-Breathing Engines Evolution.

Before getting into the Scramjet and the phenomena occurring inside, let us talk about air breathing[2] engines that it historically took place before.

Let's begin with the turboprop which is shown below, it can be used for small subsonic aircraft that means flying at a speed less than the sound velocity equal to 340 m/s and it consists of six components: the propeller which is regarded as an external component whereas the five other internal components are the inlet, the compressor, the combustor, the turbine and the nozzle. The final point is that the output Mach Number of an aircraft flying with the turboprop engine could be ranged between 0.5 and 0.75.

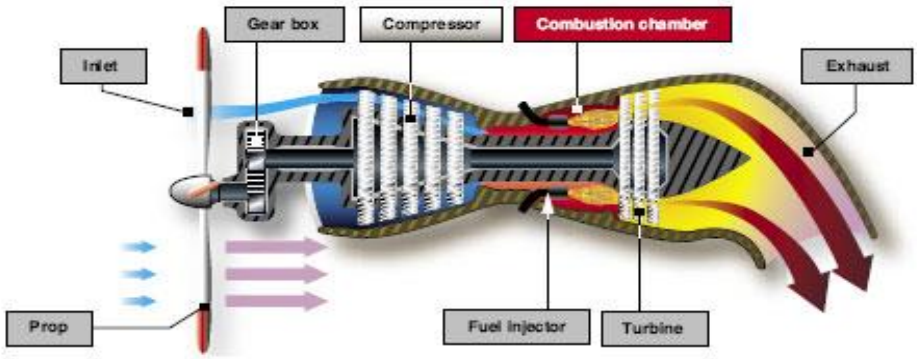

Fig.9. Turboprop Schematic Representation (Source: *www.flightlearnings.com)*

A more recent and advanced air-breathing engine which is faster and more efficient than the Turboprop is called Turbofan (represented in Fig.4) where the main difference between the latter and previous engine is that the propeller should now be an internal component located inside a duct covering the whole engine. In fact, these components play an important role which is producing more thrust allowing the aircraft to move for an output Mach number around 0.9 which is still a subsonic speed.

The figure below describes all of the recent aforementioned descriptions as such:

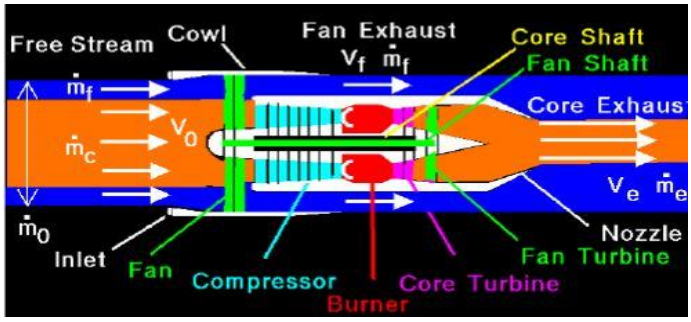

Fig.10. Turbofan Schematic Representation (Source*: www.grc.nasa.gov)*

The first air-breathing engine that could fly an airplane for a Mach number more than 1 and it may break the sound barrier as well is the Turbojet (Fig.5) where the engine's output velocity depends on the internal temperature of the turbine blades. In fact, Turbojet engines allow for a flight Mach number limit around two Machs . The concorde as well as war airplanes such as F16 are examples of aircrafts having turbojets as a flight engine.

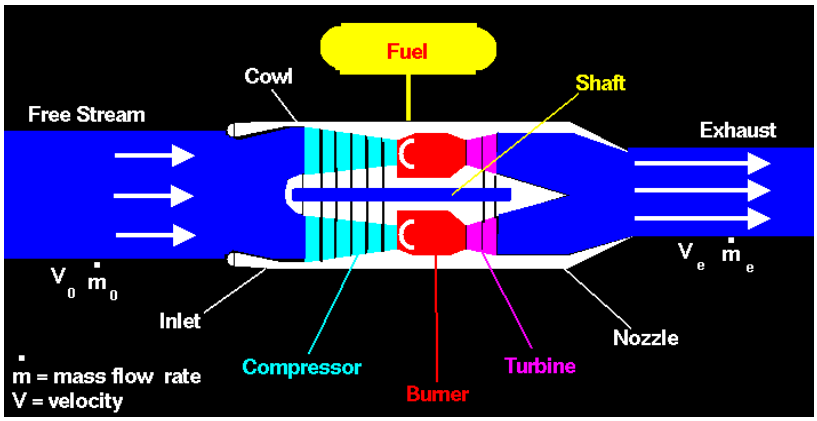

Fig.11. Turbojet Schematic Representation (Source*: www.grc.nasa.gov)*

According to the supersonic Mach numbers (above two) problems, the Turboprop, turbofan and the turbojet are not able to satisfy the problem's desire where the internal components cannot withstand the high flow temperature therefore an

improved air breathing engine is invented to fulfill the internal temperature condition discussed below.

Unlike the previous air-breathing engines mentioned above, the Ramjet shown in figure 6 consists of an inlet, an isolator, a combustion chamber and a nozzle without rotating parts such as turbines and compressors. The ramjet engine rams the incoming supersonic flow that means it compresses the air and move it into the isolator where a system of intense normal shock waves is formed called “shock train” decreasing the air flow velocity from supersonic to subsonic flow, after that it enters the combustion chamber where the heat is added to the flow by means of injectors and flame holders. Finally, the latter mixture’s energy is converted to a kinetic energy by the nozzle producing the thrust.

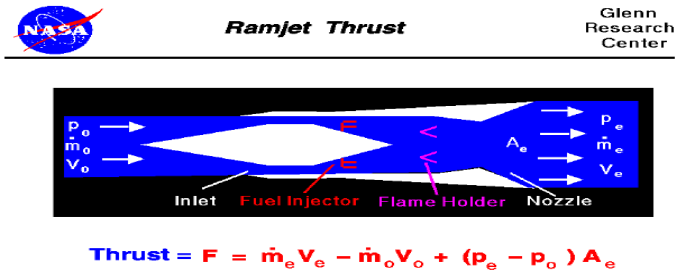

Fig.12. Ramjet Schematic Representation (Source*: www.grc.nasa.gov)*

In fact, ramjets cannot move in a static manner therefore it has to be initialized supersonically using a rocket or a turbofan such as the Turbo-ramjet engine that is used in the world fastest airplane which is the SR-71 shown below in the right hand side whereas the engine (ramjet) which makes the mentioned aircraft supersonically faster is represented in the left hand side. As a matter of fact, this engine is a turbo-ramjet which combines two modes, the turbojet is depicted on the top where the turbo-ramjet is operating in the turbojet mode. On the other hand, the engine illustrated just below the turbojet’s scheme is operated in the ramjet mode as such:

Fig.13. SR-71 TurboRamjet Schematic Representation (Source*: www.Aerospaceweb.gov)*

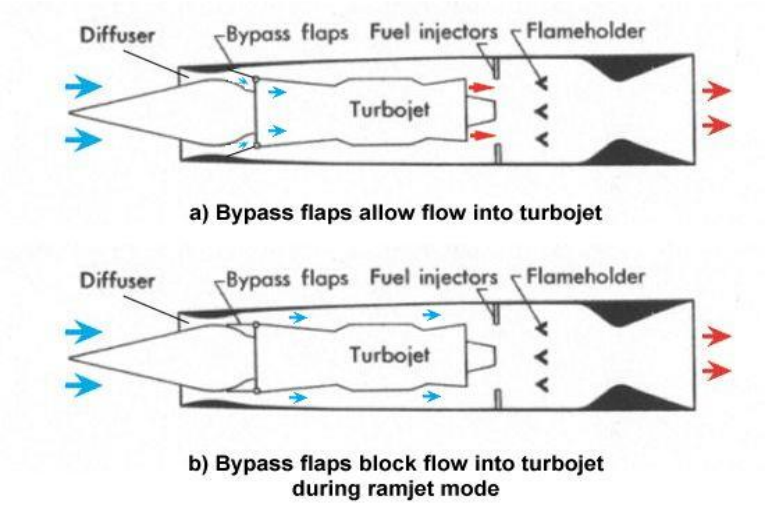

Fig.14. SR-71 (Source*: www.grc.nasa.gov)*

After having short discussions about the air-breathing engines in a general and brief form, let's get back to the main topic, Scramjets. In fact, Thomas Neuenhahn[3] points out that the scramjet engine is a ramjet where its combustion chamber operates in a

supersonic flow unlike the subsonic ramjet case where the flow entering the combustion chamber is subsonic, therefore the total pressure loss in the compression inlet part due to shock losses should be higher than that of the scramjet, that's why the scramjet is suitable for high Mach numbers, such as in the hypersonic flow (M>5).

In fact, the airflow enters the intake where it will be compressed to a specific limitation indicated by the combustion chamber. In addition, the system that consists of the compression ramps, the cowl and the isolator should lead to the minimum of total pressure and drag in order to reach the maximum thrust through the nozzle after burning the compressed air with fuel in the combustion chamber. As a matter of fact, the supersonic combustion chamber creates a high pressure backward through the subsonic part of the boundary layers leading to shockwaves creation interacting with the boundary layers to form a shock train inside the duct that separates the second compression ramp and the combustion chamber's inlet. Moreover, in case we have an increase in the supersonic pressure near the shock train, the latter would expand until it will be fallen out of the isolator leading to a normal shockwave creation in the isolator's inlet, hence a total pressure loss increase and a mass flow decrease. This kind of intake "un-start" would decrease the scramjet efficiency.

The figure below represents the hypersonic aircraft SR-72 that flies using the scramjet engine.

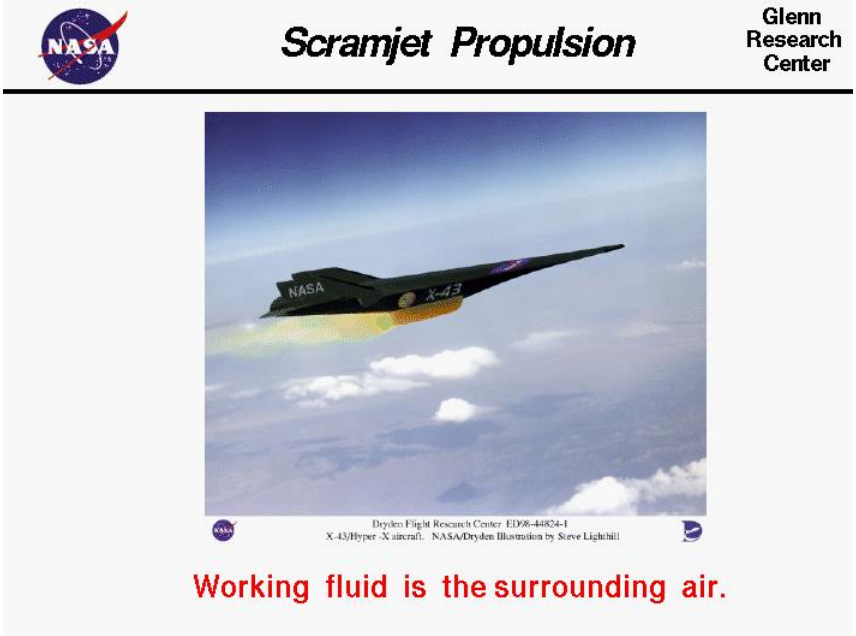

Fig.15. SR-72 (Source*: www.grc.nasa.gov)*

1.1.4 The Field of Plasma and MHD Aerodynamics

Since several examples are explained briefly about plasma natural phenomena and applications along with a quick review of the aeronautical engines evolution. Therefore it is allowed to make a short introduction about the application of plasma physics on the world of aircraft.

In general, the plasma aerodynamics field is adopted to control the shockwave intensity as well as the separation zone length within the boundary layer in a supersonic flow in order to improve the engine's efficiency. SUN Quan[4], Cui Wei and their assistants have made a numerical investigation along with an experimental validation concerning the shock boundary layer interaction control where MEMS spark dischargers are used to control the separation zone as well as the shock intensity. On the other hand, this device is placed 10mm distant from compression ramp's kink in the west direction. In fact, the plasma of the arc discharge produces a plasma layer within the boundary layer leading to a temperature higher than 1726.85 °C. Moreover, it is

experimentally observed that this plasma actuator will change the pressure and the temperature of near-wall region as well as it changes the shockwaves direction and position whereas the separation zone's area would increase. Precisely, a virtual aerodynamic ramp will be created within the actual ramp dividing the reattachment oblique shockwave into two oblique shockwaves, the reattachment oblique shockwave shifted backward as well as another induced oblique shockwave which will take the original separation's place after the breakdown of its foot.

1.2 Thesis Objective.

According to the description mentioned above about scramjets and the shock boundary layer interaction control using the MEMS plasma actuators, I have discovered that there will be severe changes for the shockwaves structures as well as for the separation zone located in the kink of the compression ramp. What if we go deep into reality and focus on natural phenomena that could or might make some changes in the SWBLI characteristics? let's imagine the natural spark discharge bombarding the separation zone instead of the MEMS arc discharger which lead of asking too many questions, why thinking of a lightning discharge ? How it would affect the surrounding supersonic parameters? What is the kind of the shockwave emanating from a thunderbolt? How does the shockwave interact with the SWBLI? I will be answering those questions where these answers will generate too many questions afterwards. In 1953, Shao-Chi Lin made an investigation about cylindrical shockwaves produced by instantaneous energy release[5] where he mentioned that the Rankine-Hugoniot jumping relations of a cylindrical shockwave could be similar to that of Taylor's spherical shockwave[6]. In fact, Shao-Chi put the approximated jumping relations where the ratio

y_1 between the pressure behind and after the shockwave which is the atmospheric pressure is too large.

But in my case, the surrounding medium is compressed so that we can use Taylor's non approximated jumping relations.

So the objective of the thesis is to model the lightning phenomena using the macroscopic method where the plasma which makes up the lightning is designed, employing the Navier-Stokes along with the Magneto-hydrodynamics equations. Moreover, the initial sudden and high temperature and pressure are the main parameters that characterize the physics of the plasmatic arc discharges. In fact, it is required to run a validated numerical simulation of a compression corner flying at a supersonic speed with a Mach Number of three interacting with the recent aforementioned long spark discharge to see through the simulated results that does not exist in the literature. So the main objective is achieved, where these results are compared to the SUNQUAN's baseline contours. Another goal to be accomplished, is to simulate the same case using additional formulae such as the Poynting flux, the variation of the magnetic field with respect to the time and the diffusion of the Lorentz force leading to a change in the structure of the shockwaves interaction system compared to the case where these formulae are not activated. Finally, theoretical formulae between the shockwaves interaction system will be represented in the Methodology section just to show the reader how these analytical equations are determined. The validations of these mathematical equations will be validated as a future work for the purpose to publish another paper, a theoretical oriented research publication.

1.3 Thesis Significance.

Filling in a literature's gap, is an essential strategy to fulfill a thesis' objective to be able to publish a paper. Furthermore, the deducted Mach number, velocity and pressure contours play an important role to improve the shockwave-shockwave interactions theory where there is a lack of information regarding the whole topic in the theoretical point of view as well as in the numerical point of view. As a matter of fact, the propagation of a strong shockwave though a pressurized medium is rarely mentioned or in other words it is implied in an indirect way. Furthermore, one of the significant thesis requirement is to model the lightning strike with its full magneto-hydrodynamics equations using ANSYS FLUENT where the second derivative is hard to be coded and implemented in the FLUENT's User Defined Functions due to the absence of the macro responsible for computing the second derivative in FLUENT leading to the achievement of another target in the literature, which is coding additional principal terms into the built in Magneto-hydrodynamics equations located in FLUENT, extracting results from them that show differences with those concluded from the original case (simple MHD equations).

1.4 Thesis Organization.

The thesis is initialized by the abstract followed by the introduction where the latter contains a historical background as well as a brief review about the space plasma physics, magneto-dynamics natural and artificial phenomena, the evolution of aircraft engines as well as the plasma applications to high supersonic aircraft. On the other hand, the following chapter will be about the literature review where so many previous research papers that are acquired and studied to gather so many information and make a

firm knowledge in order to be able to achieve all of the aforementioned objectives and to come up with new goals for the current thesis' future work.

The literature review's section is followed by the Methodology's chapter where the theoretical background will be represented along with the whole procedures and cases numerically simulated using FLUENT which leads to the results discussed in the "Results and Discussion's" chapter. Finally, the thesis will be finalized by the conclusion as well as the list of references.

CHAPTER 2

LITERATURE REVIEW

2.1 Lightning Numerical Simulation

In May 1953, it could be pointed out by Shao Chi Lin that a long electrical spar k discharge produces a strong shockwave which belongs to the cylindrical shockwaves family. Furthermore, the author affirms that Rankine-Hugoniot's Equations declared by Taylor could be theoretically used for strong shockwaves computations. In March 2014, Qiang Chen[7] and his co-authors state that Lightning Discharge is regarded as a high temperature Plasma Flow Column where it could be modeled using Compressible, Radiative , Magnetohydrodynamics equations. In addition, D.Wright and his co-authors[8] claim that the non-linearity of the electrical conductivity and ohmic heating are the main features of an electric arc discharge which took place in March, 2013. Finally, D'Angola[9] provides a way to develop the thermodynamics theoretical properties for all pressure and temperature ranges where these properties become non linear and requires formulae based on coefficients deduced by empirical or numerical procedures, such as the electrical conductivity, thermal conductivity, non ideal density for plasmas, specific heat, specific enthalpy and specific entropy, etc…So these formulae could be used to model our phenomena in a more realistic way.

2.2 Supersonic and Scramjet Simulations

Several SCRAMJET configurations are performed in the literature such as : scramjet inlets with different geometries, compression corners and double wedges located within the Scramjet Inlet and cowls geometries where several supersonic and

hypersonic effects will come into sight. In fact, Ahmet Selim Durna and his co-authors[10] performed several analysis regarding the shock-shock as well as the shockwave – boundary layer interactions taking place on a double wedge for several angles, using the Finite Volume Method and adopting the density based solver in order to simulate and visualize the resulted phenomena. It is deduced that the system of shockwaves will be modified with respect to the change of geometries such as the angle between the two connected wedges or the angle of the second neighbor wedge. As a matter of fact, when the angle reaches a critical angle of 55° there will be a creation of more than a triple point. On the other hand, complicated shockwaves interactions system become noticeable with the further increase of the angle caused by disturbances produced by the transmitted shockwave.

Edney's Classification for shock-shock interactions type is an essential sub-filed to analyze our resulted shockwaves interactions structure, where this strategy could be helpful when we particularly have a bow shock and another form of shockwaves interaction. Hongbo Lu and his co-authors[11], aim to predict the effects of the interaction of a bow shock and compression waves where a slight change in the shockwave system leads to a heat reduction. Genuinely, the contribution of Edney's strategy into the geometrical and numerical procedure and solutions provides a more obvious way to better understand the physical phenomena behind these kinds of complex interactions .According to my present research work, despite the fact that Lu's paper is so important and full of theoretical, geometrical as well as numerical details; it is just useful to better understand Edney's theories when the latter is brought into applications.

Luis F. Gutiérrez Marcantoni, José P. Tamagno and Sergio A. Elaskar [2012][12], worked on the following topic "HIGH SPEED FLOW SIMULATION USING

OPENFOAM" and their finding are – The comparison between two openFoam solvers located in the openFoam's applications library, sonicFoam and rhoCentralFoam. In fact, according to the sonicFoam solver, the adopted method is Pressure Implicit with Slitting Operators (PISO) where the pressure and velocity terms are decoupled using two main steps such as, SIMPLE algorithm due to its implicitness and the PRIME algorithm because of its stability, moreover RIEMANN numerical scheme is used to capture the supersonic flow effect (oblique shockwaves, normal shockwaves, expansion waves, etc…) and it avoids a fluctuational solution leading to an accurate result. On the other hand, in rhoCentralFoam the computation of the interpolation fluxes is required where flow and propagation of waves properties are taken into account, furthermore, high resolution central scheme are used (Kurganov and Tadmor, 2000)[13] as an alternative numerical approach instead of RIEMANN. Finally, the three authors achieve with a result where rhoCentralFoam is better suited for compressible flow computations knowing that sonicFoam is using the PISO method where the latter is originally made for incompressible purposes and then modified to be compatible with compressible problems.

C. Fureby, M. Chapuis, E. Fedina & J. Tegnér [2010][14], worked on a topic which is "A COMPUTATIONAL STUDY OF SCRAMJET COMBUSTION" where their main objective – Is to make a numerical LES combustion proof and verification using a software called OpenFoam applied to two combustors, the laboratory supersonic combustor and the Hyshot II. Beside the LES solver, the mixed subgrid scale flow model[15] and the Partially Stirred Reaction turbulence chemistry interaction (paSR)[16] are used along with a two-stage Runge-Kutta time-Integration scheme and these solvers are located in the OpenFoam library that could be modified to be well suited and

compatible with the desired problem requirements moreover the combination of these numerical methods provide us a deeper insight about supersonic air-fuel mixing as well as a better understanding of the pressure, velocity and heat distribution inside the combustor and through the H_2 injectors. Finally, this study lead us to cope with supersonic flow effects on combustion which is important for the scramjet improvements and advanced new technology.

YUFENG YAO and DANIEL RINCON [2012][17],worked on the topic "SHOCK INDUCED SEPARATING FLOWS IN SCRAMJET INTAKES" and their research – Is studying the supersonic flow through the intake of a scramjet "Reinartz et al.(2006)" model where the effects of the oblique shock – boundary layer interaction leading to a flow separation are simulated using ANSYS and then compared to an experimental data.

YAO and RINCON focus was the CFD prediction of the wall pressure coefficient distribution C_p using unstructured mesh without cowl wedge; structured mesh without cowl wedge and structured grid with cowl wedge then based on this study, the significance of the shockwave existence is shown where it affects the current thermophysical properties differently whether the cowl wedge is removed. Moreover, eight types of turbulence model has been studied as well as wall skin friction and heat transfer coefficient distribution are computed using some turbulence model to capture the separation bubble where each model predict a certain bubble dimension, after that, Mach number and velocity contours are represented around the bubble. Finally, the authors made a comparison of wall pressure and skin friction coefficient distribution between sharp and round leading-edge. In fact, in the case of a rounded shape; we have

a larger bubble which makes the flow harder to move forward decreasing the scramjet engine performance.

W. Schuyler Hinman, Craig T. Johansen, Chris J. Arisman, Wagner C. Galuppo [2014][18] worked on the following topic "Numerical Investigation of Laminar Near Wake Seperation On Circular Cylinders at Supersonic Velocities" and their objectives – Investigating and simulating the supersonic flow over a cylinder using OpenFoam where the compressible solver located in the OpenFoam library rhoCentralFoam is used. In fact, the existence of shocks induce a boundary layer separation then its re-attachment leading to a re-circulating flow zone where this phenomena and all kinds of physics related to the supersonic effects on the cylinder are post-processed and visualized through paraFoam. Generally, compressor corners designed for a scramjet intake has the same general physical background, so for a better understanding of the separation mechanism, supersonic flow is simulated for a wide Mach and Reynolds number ranges compared to experimental data where it denotes that Mach and Reynolds numbers are interdependent.

Lt Col Troy C. Hoeger, Dr. Paul I. King, and Lt Col Douglas D. Decker [2010][19], worked on a topic which is about "CFD Modeling of an Isolator Shock Train in a Scramjet Engine" where their research was – Pre-Combustion Shock Train (PSCT) simulation and investigation using the VULCAN code. In fact, the appearance of PSCT is significant in a dual-mode scramjet while getting into ram to scram mode transition where for high-Mach number the PSCT disappears. In the combustion process, the inlet pressure is generally lower than that of the combustor therefore we have a shockwave propagation through the isolator which is nothing but a duct starting from an oblique shockwave at the end inlet point.

The produced shock train is characterized by a length where the latter depends in the isolator geometrical features and the pressure ratio between the combustor and inlet. On the other hand, the back pressure due to high combustion leading to a shock train has a negative effects on the scramjet engine efficiency. Therefore the main focus of this article is to simulate and visualize the influence of this back pressure on the length and the coordinates of the PSCT inside the isolator to cope with the problem and improve the scramjet performance.

Sudharsan, N.M, Jambekhar, V.A and Babu V [2010][20], has worked on "A validation study of OpenFOAM using the supersonic flow in a mixed compression intake" where their research was – studying supersonic and hypersonic flow through several compression intake geometrical configurations using OpenFOAM where this kind of CFD software could replace experimental operations which are regarded too expensive. These authors show the importance of such an open source where comparisons have been made between numerical simulations and results achieved by previous works and experiments. In fact, these authors have adopted the sonicTurboFoam as a main solver to perform the simulations knowing that unlike rhoCentralFoam and sonicFoam, the viscous effect could be involved as well as the RNG k-ε turbulence model is included where the latter is compatible with supersonic and hypersonic flow features. The numerical simulations made by the authors match the previous experimental results but there is an unexpected additional characteristic that exists which is the presence of oscillations around shockwaves. On the other hand, the authors mentioned the requirement of the angle of attack variations starting from Mach Number > 1.2 to hypersonic Mach Numbers in order to test this open source code and to

notice if the latter could be regarded as an expensive experimental procedure substitution or not.

Ramesha D.K., Rudra Murthy, Hemanth Kumar.P [2013][21], woked on " CFD Analysis of Supersonic Exhaust in a Scramjet Engine" where their research was – a CFD based prediction and investigation of supersonic flow through the nozzle or exhaust of a scramjet using ANSYS FLUENT. In fact the upperwall of the exhaust nozzle consist of a cowl and a wedge beside whereas the lower wall is nothing but a twenty degree inclined after-body where pressure and temperature contours along the twenty degree inclined after-body with wedge are plotted as well as the variation of pressure along the after-body is plotted with respect to the horizontal distance. Moreover, the simulated static pressure distribution and the total heat flux along the twenty degree inclined after-body with wedge are plotted with respect to the horizontal distance and compared with the experimental data where experimental procedure and the predictions are matched.

Karri Simachalam Naidu and Dinesh Kumar Bajaj [2013][22] has worked on "Modeling and Exhaust Nozzle Flow Simulations in a Scramjet " where their focus was – The same research procedure as the previous article " CFD Analysis of Supersonic Exhaust in a Scramjet Engine". In fact, these authors made the same plots and comparisons using ANSYS FLUENT as well for the same parameters used before but they added the zero angle after-body as a lower wall for the exhaust and they performed their predictions with an without the wedge located in the upper wall. Moreover, as for the previous article the authors mentioned the significance of the generated shockwaves effects on the specified parameters where they are shown in the plots.

CHAPTER 3

THEORY AND METHODOLOGIES

Assume that the natural lightning discharge will strike the intake of the scramjet through the boundary layer for a distance of 10mm approx from the kink of the compression ramp in the west direction so that the cylindrical shockwave due to lightning will be interacting the system of reattachment and separation shockwaves in the upper zone as well as the boundary layer and its characteristics in the lower zone.

Let's begin with the reattachment-separation shockwave system which is regarded as an oblique shockwave, therefore the theoretical study below is about the oblique shockwave-cylindrical shockwave interaction or in other words, it is about the propagation of a cylindrical shockwave in a compressed medium.

The following figure will be describing and clarifying the short discussion above in order to introduce the concept of the thesis and to let the reader better understand the procedure and the mechanism of the shockwaves interaction system applied on the scramjet inlet's compression corner or ramp.

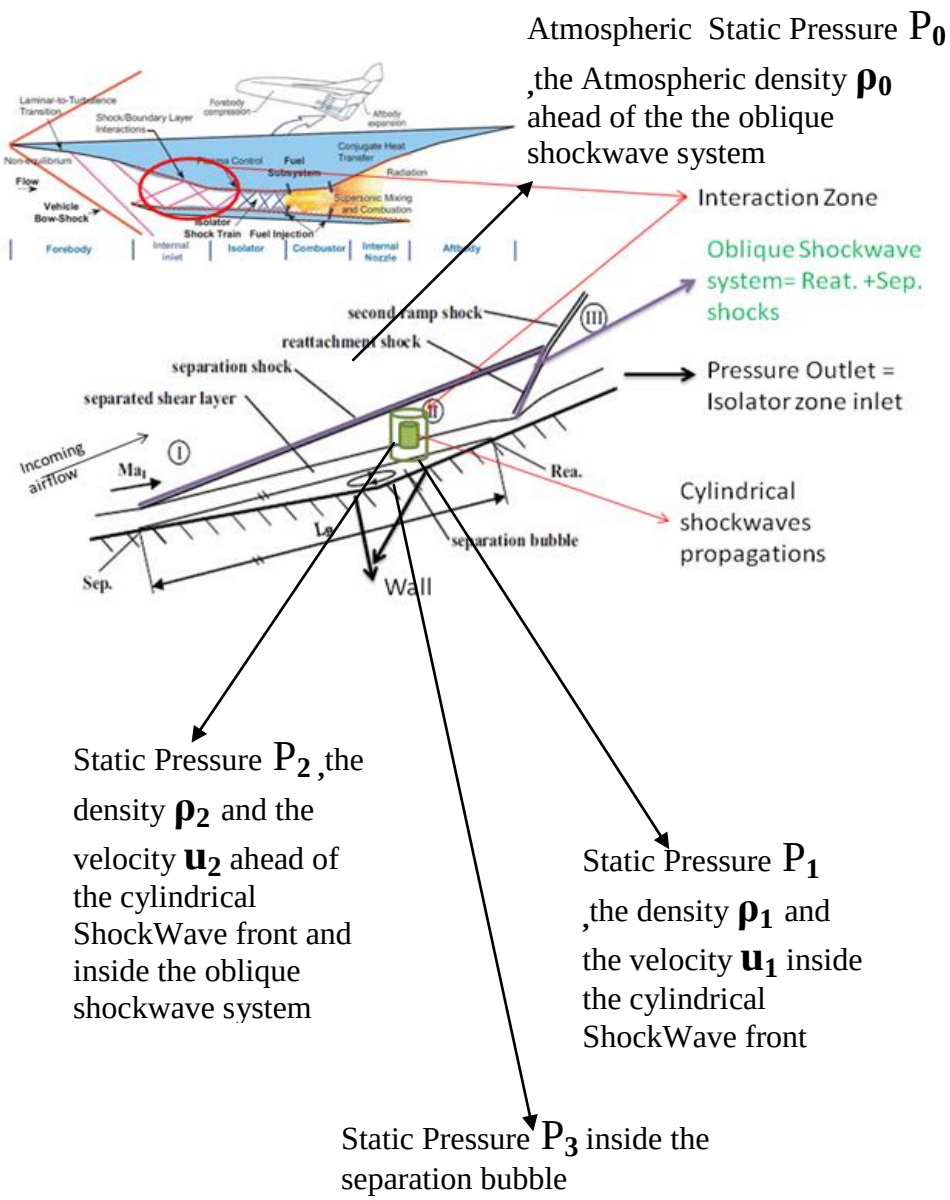

Fig.16. Concept of the Thesis' Scheme.

3.1 Theoretical Background

The following three equations represent the Rankine-Hugoniot jump conditions mentioned by Taylor and briefly discussed in the literature review chapter, for $\mathbf{y_1=P_1/P_2}$ where y_1 is not too large so it cannot be neglected.

$$\frac{\rho_1}{\rho_0} = \frac{\gamma-1+(\gamma+1)y_1}{\gamma+1+(\gamma-1)y_1},$$
$$\frac{U^2}{a^2} = \frac{1}{2\gamma}\{\gamma-1+(\gamma+1)y_1\}, \qquad \textbf{(3.1)}$$
$$\frac{u_1}{U} = \frac{2(y_1-1)}{\gamma-1+(\gamma+1)y_1},$$

In fact, Taylor used the approximated formulae where he regards y_1 is too large due to the gap between the region behind the blast wave and ahead of the shock wave front leading to specific results lacking a little of accuracy, so why not improving the accuracy of the results and generalizing it by developing generalized formulae using the jumping conditions (3.1) that are mentioned in Taylor's paper. On the other hand, Taylor didn't reveal the theoretical derivation and resources of equations (3.1) but **in general**, jumping conditions are derived using Navier Stokes and state equations. Since y_1 cannot be neglected then we can consider that P_2 is the compressed region due to the oblique shockwave, P_1 is the compressed region due to the blast wave and P_0 is the uncompressed region or ambient air where it will be replaced by the following oblique shockwave equations. Hence, equation (3.1) becomes as such:

$$\frac{\rho_1}{\rho_2} = \frac{\gamma-1+(\gamma+1)y_1}{\gamma+1+(\gamma-1)y_1} \qquad \textbf{(3.2a)}$$

$$\frac{U^2}{a^2} = \frac{1}{2\gamma}\{\gamma - 1 + (\gamma + 1)y_1\} \quad \textbf{(3.3b)}$$

$$\frac{u_1}{U} = \frac{2(y_1 - 1)}{\gamma - 1 + (\gamma + 1)y_1} \quad \textbf{(3.4c)}$$

where the variables ρ_1, ρ_2 represent the density just before the blast wave and ahead of the blast wave front located in the compressed region respectively.

Variables "u_1" and "U" represent the particles velocity just before the blast wave and the velocity of the blast wave front respectively.

The parameter "a"; represents the sound velocity in the compressed region ahead of the blast wave front.

In fact, to be able to express the pressure just before the blast wave front $\mathbf{P_1}$ in terms of the ambient uncompressed pressure P_0 as well as for the density case, the oblique shockwave equations are required.

The general oblique shockwave relations[23] are expressed as such:

$$\frac{\rho_2}{\rho_0} = \frac{(\gamma + 1)M_1^{\,2}\sin^2\beta}{2 + (\gamma - 1)M_1^{\,2}\sin^2\beta} \quad \textbf{(3.5)}$$

$$\frac{P_2}{P_0} = 1 + \frac{2\gamma}{\gamma + 1}(M_1^{\,2}\sin^2\beta - 1) \quad \textbf{(3.6)}$$

Where $M_{1n} = M_1^{\,2}\sin^2\beta$ is the normal component of the first upstream Mach number M_1.

β is the oblique shock wave angle.

P_0 and ρ_0 represent the pressure and the density in the non compressed ambient air respectively.

equation **(3.4)** becomes :

$$\frac{P_2}{P_0} = \frac{2\gamma M_{1n}{}^2 - (\gamma - 1)}{\gamma + 1} \qquad \textbf{(3.7)}$$

Now I have to determine $\boldsymbol{\rho_1 / \rho_2 = ?}$. From **(3.2a)** we have,

$$\frac{\rho_1}{\rho_2} = \frac{\gamma - 1 + (\gamma + 1)\dfrac{P1}{P2}}{\gamma + 1 + (\gamma - 1)\dfrac{P1}{P2}} \qquad \textbf{(3.8)}$$

Let's replace P_2 by its theoretical value from equation **(3.5)**, **P1/P2** will be expressed as such:

$$\frac{P_1}{P_2} = \frac{P_1}{\dfrac{2\gamma M_{1n}{}^2 - (\gamma - 1)}{\gamma + 1} P_0} \qquad \textbf{(3.9)}$$

$$\frac{P_1}{P_2} = \frac{\gamma + 1}{2\gamma M_{1n}{}^2 - (\gamma - 1)} \frac{P_1}{P_0} \qquad \textbf{(3.10)}$$

Therefore equation **(3.7)** becomes :

$$\frac{\rho_1}{\rho_2} = \frac{\gamma - 1 + (\gamma + 1)\left(\frac{\gamma + 1}{2\gamma M_{1n}{}^2 - (\gamma - 1)}\right)\frac{P_1}{P_0}}{\gamma + 1 + (\gamma - 1)\left(\frac{\gamma + 1}{2\gamma M_{1n}{}^2 - (\gamma - 1)}\right)\frac{P_1}{P_0}} \qquad \textbf{(3.11)}$$

Let's make **(3.9)** a compact formula as such :

$$\frac{\rho_1}{\rho_2} = \frac{[(2\gamma M_{1n}{}^2 - (\gamma - 1))(\gamma - 1)] + (\gamma + 1)^2 \frac{P_1}{P_0}}{[(2\gamma M_{1n}{}^2 - (\gamma - 1))(\gamma + 1)] + (\gamma^2 - 1)\frac{P_1}{P_0}} \qquad \textbf{(3.12)}$$

In order to express ρ_1 in terms of a known density which is ρ_0 , let's replace **(3.4)** into the left side of equation **(3.11)** which becomes **:**

$$\frac{\rho_1}{\rho_0} = \frac{[(\gamma + 1)M_{1n}{}^2]\{[(2\gamma M_{1n}{}^2 - (\gamma - 1))(\gamma - 1)] + (\gamma + 1)^2 \frac{P_1}{P_0}\}}{[2 + (\gamma - 1)M_{1n}{}^2]\{[(2\gamma M_{1n}{}^2 - (\gamma - 1))(\gamma + 1)] + (\gamma^2 - 1)\frac{P_1}{P_0}\}} \qquad \textbf{(3.13)}$$

Hence the first Modified Rankine-Hugoniot jumping equation is obtained.

Let's modify the second Rankine-Hugoniot equation, starting from **(3.3b)** where in this case "a" is the velocity of the sound in the compressed air behind the oblique shockwave.

$$a = \sqrt{\gamma RT} = \sqrt{\frac{\gamma P_2}{\rho_2}} \tag{3.14}$$

Equation **(3.3b)** becomes :

$$\frac{U^2}{(\sqrt{\frac{\gamma P_2}{\rho_2}})^2} = \frac{1}{2\gamma}\{(\gamma-1) + \frac{(\gamma+1)^2}{[2\gamma M_{1n}^2 - (\gamma-1)]} \tag{3.15}$$

Using **(3.4)** and **(3.5),** a^2 could be determined as such:

$$\frac{\gamma P_2}{\rho_2} = \frac{[2\gamma M_{1n}^2 - (\gamma-1)]}{(\gamma+1)} \frac{[2+(\gamma-1)M_{1n}^2]}{(\gamma+1)M_{1n}^2} (\frac{\gamma P_0}{\rho_0}) \tag{3.16}$$

where $a_0 = \frac{\gamma P_0}{\rho_0}$ represent the velocity of the sound in the uncompressed ambient air.

Therefore the second modified Rankine-Hugoniot equation becomes **(3.16)**

$$\frac{U^2}{a_0^2} = \{\frac{1}{2\gamma}\{(\gamma-1) + \frac{(\gamma+1)^2}{[2\gamma M_{1n}^2 - (\gamma-1)]} \frac{P_1}{P_0}\}\}\{\frac{[2\gamma M_{1n}^2 - (\gamma-1)]}{(\gamma+1)} \frac{[2+(\gamma-1)M_{1n}^2]}{(\gamma+1)M_{1n}^2}\} \tag{3.17}$$

Finally, let's take the third Rankine-Hugoniot equation **(3.3c)** and let's modify it as such:

$$\frac{u_1}{U} = \frac{2\{\frac{(\gamma+1)}{(2\gamma M_{1n}^2 - (\gamma-1))} \frac{P_1}{P_0} - 1\}}{(\gamma-1) + (\gamma+1) \frac{(\gamma+1)}{(2\gamma M_{1n}^2 - (\gamma-1))} \frac{P_1}{P_0}} \tag{3.18}$$

$$\frac{u_1}{U} = \frac{2[(\gamma+1)\frac{P_1}{P_0} - (2\gamma M_{1n}^2 - (\gamma-1))]}{(\gamma-1)(2\gamma M_{1n}^2 - (\gamma-1)) + (\gamma+1)^2 \frac{P_1}{P_0}} \qquad \textbf{(3.19)}$$

Hence, the third Modified Rankine-Hugoniot equation is obtained where u_1 the velocity of the particles just behind the blast wave front.

Let's focus on equation **(3.15)**, I can deduce that **P_1/P_0** could be expressed in terms of known values (γ,M_{1n},U,a_0 and $P_{0)}$.

Equation **(3.16)** could be written in the following form:

$$\frac{\frac{U^2}{a_0^2}}{\{\frac{[2\gamma M_{1n}^2 - (\gamma-1)]}{(\gamma+1)} \frac{[2+(\gamma-1)M_{1n}^2]}{(\gamma+1)M_{1n}^2}\}} = \frac{1}{2\gamma}\{(\gamma-1) + \frac{(\gamma+1)^2}{[2\gamma M_{1n}^2 - (\gamma-1)]}\frac{P_1}{P_0}\} \qquad \textbf{(3.20)}$$

Moving **P_1/P_0** to the left side, we obtain equation **(3.20):**

$$\frac{P_1}{P_0} = \{2\gamma[\frac{U^2}{a_0^2}\frac{(\gamma+1)^2 M_{1n}^2}{[2\gamma M_{1n}^2 - (\gamma-1)][2+(\gamma-1)M_{1n}^2]}] - (\gamma-1)\}\frac{[2\gamma M_{1n}^2 - (\gamma-1)]}{(\gamma+1)^2} \qquad \textbf{(3.21)}$$

Hence, the distribution of the pressure just behind the blast wave front is obtained in terms of known variables mentioned before.

In order to get the density ρ_1 just behind the blast wave front, we can replace equation **(3.20) into (3.12).**

Moreover, to be able to get the velocity of particles u_1 just behind the blast wave front, we can replace equation **(3.20) into (3.18).**

The blast wave velocity "U" could be assumed in terms of the first downstream Mach number M_2 (the second upstream Mach number in the compressed region), in terms of a constant velocity U_2 for a specific shockwave radius R_2 and in terms of a variable Radius R.

According to the lower part, the cylindrical shockwave will be interacting the zone between the separation and the reattachment shockwaves where its pressure equation is given by equation (3.1) in terms of the pressure of the first ramp surroundings, so that let's replace the pressure distribution of this zone to the Rankine-Hugoniot equations (3.2).

let's assume that P_1 is the pressure just behind the cylindrical shockwave front and P_3 is the pressure ahead of the front that means the separated zone which is given in equation (3.1).

$$\frac{P_1}{P_3} = \frac{P_1}{\{1+0.5M^2{}_1\gamma F(2c_{f,0})^{0.5}(M^2{}_1-1)^{-0.25}\}P_I} \quad \textbf{(3.22)}$$

$$a^2 = \gamma RT = \frac{\gamma P_3}{\rho_3} = \frac{\gamma\{1+0.5M^2{}_1\gamma F(2c_{f,0})^{0.5}(M^2{}_1-1)^{-0.25}\}P_I}{\rho_3} \quad \textbf{(3.23)}$$

Where a represent the speed of sound inside the separated zone.

Replacing (3.22) into (3.2b) in order to get the pressure behind the strong shockwave front we will get:

$$P_1 = \frac{[2U^2\rho_3 - [\{1+0.5M^2{}_1\gamma F(2c_{f,0})^{0.5}(M^2{}_1-1)^{-0.25}\}P_I(\gamma-1)]]}{\gamma+1} \quad \textbf{(3.24)}$$

Let's replace (3.21) into (3.2a) and (3.2c) we will get:

$$\frac{\rho_1}{\rho_3}=\frac{\gamma-1+(\gamma+1)\{\dfrac{[2U^2\rho_3-[\{1+0.5M^2{}_1\gamma F(2c_{f,0})^{0.5}(M^2{}_1-1)^{-0.25}\}P_I(\gamma-1)]]}{\gamma+1}\}}{\gamma+1+(\gamma-1)\{\dfrac{[2U^2\rho_3-[\{1+0.5M^2{}_1\gamma F(2c_{f,0})^{0.5}(M^2{}_1-1)^{-0.25}\}P_I(\gamma-1)]]}{\gamma+1}\}} \quad \textbf{(3.25)}$$

$$\frac{u_1}{U}=\frac{2(\{\dfrac{[2U^2\rho_3-[\{1+0.5M^2{}_1\gamma F(2c_{f,0})^{0.5}(M^2{}_1-1)^{-0.25}\}P_I(\gamma-1)]]}{\gamma+1}\}-1)}{\gamma-1+(\gamma+1)\{\dfrac{[2U^2\rho_3-[\{1+0.5M^2{}_1\gamma F(2c_{f,0})^{0.5}(M^2{}_1-1)^{-0.25}\}P_I(\gamma-1)]]}{\gamma+1}\}} \quad \textbf{(3.26)}$$

Where P_I, Ma_I, γ, F, $C_{f,0}$, ρ_2 are known parameters.

P_1 and u_1 are the variables to be computed and compared with the validation done by ANSYS FLUENT, then the results will be published as a second research paper along with the thesis' publication paper.

3.2 Governing Equations.

Before getting into the Computational Fluid Dynamics (C.F.D) 's numerical methodology, it is required to focus on the governing equations as well as their derivation in order to clarify what is mathematically behind the phenomena occurring in the thesis' case study.

The mass conservation equation or in other terms the continuity equation is governed to analytically describe that the input of the mass flux should be equal to the mass flux output in addition to the accumulation term providing we have a transient problem.

Here, the continuity equation is written in the non conservative form as such:

$$\frac{\partial \rho}{\partial t} + \vec{\nabla}.\left(\rho\vec{U}\right) = 0 \qquad \textbf{(3.27)}$$

where the density is not constant due to the flow which is travelling at a speed that exceeds the sound velocity.

The non conservative form of the momentum equation could be written in this fashion:

$$\rho\frac{\partial \vec{U}}{\partial t} + \left(\rho\vec{U}.\vec{\nabla}\right)\vec{U} = -\vec{\nabla}P + \vec{J} \times \vec{B}\,; \qquad \textbf{(3.28)}$$

Where $\vec{J}$ represents the density current with a unit of A/m;

$\vec{B}$ represents the magnetic field with a unit of Tesla (T);

$\vec{J} \times \vec{B}$ represents the Lorentz force with a unit of Newton (N);

Equation (3.28) could be expressed in this form:

$$\frac{\partial\left(\rho\vec{U}\right)}{\partial t} + \vec{\nabla}.\left(\rho\vec{U}\vec{U}\right) - \vec{U}\left(\frac{\partial \rho}{\partial t} + \vec{\nabla}.\left(\rho\vec{U}\right)\right) = -\vec{\nabla}P + \vec{J} \times \vec{B};$$

Since $\rho\frac{\partial \vec{U}}{\partial t} = \frac{\partial\left(\rho\vec{U}\right)}{\partial t} - \frac{\vec{U}\,\partial \rho}{\partial t}$;

And $\left(\rho\vec{U}.\vec{\nabla}\right)\vec{U} = \vec{\nabla}.\left(\rho\vec{U}\vec{U}\right) - \vec{U}\vec{\nabla}.\left(\rho\vec{U}\right)$;

In fact, the Lorentz Force is nothing but:

$$\vec{J} \times \vec{B} = \frac{1}{\mu_0}\left(\vec{\nabla} \times \vec{B}\right) \times \vec{B};$$

$$\vec{J} \times \vec{B} = \frac{1}{\mu_0}\vec{\nabla}\left(\vec{B}.\vec{B}\right) - \frac{1}{\mu_0}\left(\vec{\nabla}.\vec{B}\right)\vec{B} - \vec{\nabla}\left(\frac{B^2}{2\mu_0}\right);$$

Where $\left(\vec{\nabla}\times\vec{\mathrm{B}}\right)\times\vec{\mathrm{B}}=\left(\vec{\mathrm{B}}.\vec{\nabla}\right)\vec{\mathrm{B}}-\vec{\nabla}\left(\frac{\mathrm{B}^2}{2}\right);$

And $\left(\vec{\mathrm{B}}.\vec{\nabla}\right)\vec{\mathrm{B}}=\vec{\nabla}.\left(\vec{\mathrm{B}}\vec{\mathrm{B}}\right)-\left(\vec{\nabla}.\vec{\mathrm{B}}\right)\vec{\mathrm{B}};$

Hence the Lorentz force development leads to the complete magneto-hydrodynamics momentum equation (3.29) as such:

$$\frac{\partial(\rho\vec{\mathrm{U}})}{\partial\mathrm{t}}+\vec{\nabla}.\left(\rho\vec{\mathrm{U}}\vec{\mathrm{U}}\right)-\vec{\mathrm{U}}\left(\frac{\partial\rho}{\partial\mathrm{t}}+\vec{\nabla}.\left(\rho\vec{\mathrm{U}}\right)\right)=-\vec{\nabla}\mathrm{P}+\frac{1}{\mu_0}\vec{\nabla}\left(\vec{\mathrm{B}}.\vec{\mathrm{B}}\right)-\frac{1}{\mu_0}\left(\vec{\nabla}.\vec{\mathrm{B}}\right)\vec{\mathrm{B}}-\vec{\nabla}\left(\frac{\mathrm{B}^2}{2\mu_0}\right); \quad \textbf{(3.29)}$$

According to the Energy equation, it is recommended to mathematically describe the whole equation by dividing it into three parts, the internal energy equation, the kinetic energy equation as well as the magnetic energy equation in order to better understand the entire derivation of the equation.

Let's begin with the Internal energy equation which is expressed in the following way:

$$\frac{\partial(\rho\mathrm{e})}{\partial\mathrm{t}}+\vec{\nabla}.\left(\rho\vec{U}e\right)-e\left(\frac{\partial\rho}{\partial t}+\vec{\nabla}.\left(\rho\vec{U}\right)\right)=-P\vec{\nabla}.\vec{U}+\eta\vec{J}^2; \quad \textbf{(3.30)}$$

Knowing that "η" is the resistivity of the conducting fluid having (Ω.m) as a SI unit.

The term $\eta\vec{J}^2$ represents the joule effect of the sudden high temperature fluid.

Multiplying the velocity vector to equation (3.28) to generate the Kinetic Energy Equation:

$$\frac{\partial\left(\frac{1}{2}\rho U^2\right)}{\partial t}+\vec{\nabla}.\left(\frac{1}{2}\rho U^2\vec{U}\right)-\frac{1}{2}U^2\left(\frac{\partial\rho}{\partial t}+\vec{\nabla}.\left(\rho\vec{U}\right)\right)=-\vec{U}.\vec{\nabla}P+$$

$$\vec{U}.\left(\frac{1}{\mu_0}\vec{\nabla}\left(\vec{B}.\vec{B}\right)-\frac{1}{\mu_0}\left(\vec{\nabla}.\vec{B}\right)\vec{B}-\vec{\nabla}\left(\frac{B^2}{2\mu_0}\right)\right); \quad \textbf{(3.31)}$$

On the other hand, it is required to make the dot product between the magnetic field and the Faraday's law to obtain the magnetic energy equation as such:

$$\frac{\vec{B}}{\mu_0}.\left(\frac{\partial\vec{B}}{\partial t}+\vec{\nabla}\times\vec{E}\right)=0;$$

$$\left(\frac{\partial\left(\frac{B^2}{2\mu_0}\right)}{\partial t}+\frac{\vec{B}}{\mu_0}.\left(\vec{\nabla}\times\vec{E}\right)\right)=0;$$

$$\frac{\partial\left(\frac{B^2}{2\mu_0}\right)}{\partial t}+\frac{\vec{E}}{\mu_0}.\left(\vec{\nabla}\times\vec{B}\right)+\frac{\vec{\nabla}}{\mu_0}.\left(\vec{E}\times\vec{B}\right)=0;$$

$$\frac{\partial\left(\frac{B^2}{2\mu_0}\right)}{\partial t}+\vec{E}.\vec{J}+\frac{\vec{\nabla}}{\mu_0}.\left(\vec{E}\times\vec{B}\right)=0;$$

The electric field is given by Ohm's law by the following expression:

$$\vec{E}=\ \eta\vec{J}-\vec{U}\times\vec{B};$$

Making the vector product of the ohms law terms by the magnetic field vector:

$$\vec{E}\times\vec{B}=\ \eta\vec{J}\times\vec{B}-(\vec{U}\times\vec{B})\times\vec{B};$$

Using the vectors identities the second term of the above equation could be written:

$$\left(\vec{\mathrm{U}} \times \vec{\mathrm{B}}\right) \times \vec{B} = \left(\vec{\mathrm{U}}.\vec{\mathrm{B}}\right)\vec{B} - B^2\vec{U}$$

Adding the Lorentz force term derived and developed above:

$$\vec{\mathrm{J}} \times \vec{\mathrm{B}} = \frac{1}{\mu_0}\vec{\nabla}\left(\vec{\mathrm{B}}.\vec{\mathrm{B}}\right) - \frac{1}{\mu_0}\left(\vec{\nabla}.\vec{\mathrm{B}}\right)\vec{\mathrm{B}} - \vec{\nabla}\left(\frac{\mathrm{B}^2}{2\mu_0}\right);$$

Therefore expression of $\vec{\mathrm{E}} \times \vec{B}$ could be reached along with the term carrying the dot product of the electric field with the density current where the Ohm's law is multiplied by the current density to get the term $\vec{\mathrm{E}}.\vec{\mathrm{J}} = \eta J^2 - \vec{J}.\left(\vec{\mathrm{U}} \times \vec{\mathrm{B}}\right);$

So let's group all of the above terms to build up the Magnetic Energy Equation as follows:

$$\frac{\partial\left(\frac{\mathrm{B}^2}{2\mu_0}\right)}{\partial \mathrm{t}} + \eta J^2 - \vec{J}.\left(\vec{\mathrm{U}} \times \vec{\mathrm{B}}\right) + \frac{\vec{\nabla}}{\mu_0}.\left(\frac{\eta}{\mu_0}\vec{\nabla}\left(\vec{\mathrm{B}}.\vec{\mathrm{B}}\right)\right) - \frac{\vec{\nabla}}{\mu_0}.\left(\frac{\eta}{\mu_0}\left(\vec{\nabla}.\vec{\mathrm{B}}\right)\vec{\mathrm{B}}\right) -$$

$$\frac{\vec{\nabla}}{\mu_0}.\vec{\nabla}\left(\eta\frac{\mathrm{B}^2}{2\mu_0}\right) - \frac{\vec{\nabla}}{\mu_0}.\left(\vec{\mathrm{B}}\left(\vec{\mathrm{U}}.\vec{\mathrm{B}}\right)\right) + \vec{\nabla}\left(\frac{\mathrm{B}^2}{\mu_0}\vec{\mathrm{U}}\right) = 0; \qquad \textbf{(3.32)}$$

Finally, the accumulation of the Internal Energy, the Kinetic Energy and the Magnetic Energy terms generates the Total Energy Equation as formulated below:

$$\frac{\partial\left(\rho e+\frac{1}{2}\rho U^2+\frac{B^2}{2\mu_0}\right)}{\partial t}+\vec{\nabla}.\left(\rho\vec{U}e+\frac{1}{2}\rho U^2\vec{U}+\vec{U}\left(\frac{B^2}{2\mu_0}\right)\right)$$

$$-e\left(\frac{\partial\rho}{\partial t}+\vec{\nabla}.\left(\rho\vec{U}\right)\right)-\frac{1}{2}U^2\left(\frac{\partial\rho}{\partial t}+\vec{\nabla}.\left(\rho\vec{U}\right)\right)$$

$$+\frac{\vec{\nabla}}{\mu_0}.\left(\frac{\eta}{\mu_0}\vec{\nabla}\left(\vec{B}.\vec{B}\right)\right)-\frac{\vec{\nabla}}{\mu_0}.\left(\frac{\eta}{\mu_0}\left(\vec{\nabla}.\vec{B}\right)\vec{B}\right)$$

$$-\frac{\vec{\nabla}}{\mu_0}.\vec{\nabla}\left(\eta\frac{B^2}{2\mu_0}\right)-\frac{\vec{\nabla}}{\mu_0}.\left(\vec{B}\left(\vec{U}.\vec{B}\right)\right)$$

$$=-P\vec{\nabla}.\vec{U}-\vec{U}.\vec{\nabla}P-\vec{\nabla}\left(\frac{B^2}{2\mu_0}\vec{U}\right);$$

(3.33)

The final equation to derive is the Magnetic Induction equation where the Ohm's law is developed through the Faraday's law in the following way.

$$\frac{\partial\vec{B}}{\partial t}+\vec{\nabla}\times\vec{E}=0;$$

$$\frac{\partial\vec{B}}{\partial t}+\vec{\nabla}\times\left(\eta\vec{J}\right)-\vec{\nabla}\times\left(\vec{U}\times\vec{B}\right)=0;$$

If the resistivity η is not spatially uniform, the curl of the product of the density current vector and the resistivity could be written in this fashion.

$$\vec{\nabla} \times (\eta \vec{J}) = \frac{1}{\mu_0} \vec{\nabla} \times (\eta \vec{\nabla} \times \vec{B})$$

$$= \frac{1}{\mu_0} \vec{\nabla} \times \left(\vec{\nabla} \times (\eta \vec{B})\right) - \frac{1}{\mu_0} \vec{\nabla} \times \left(\vec{\nabla} \eta \times \vec{B}\right);$$

$$\vec{\nabla} \times (\eta \vec{J})$$

$$= \frac{1}{\mu_0} (\vec{\nabla} \left(\vec{\nabla}. (\eta \vec{B})\right) - \vec{\nabla}^2 (\eta \vec{B}) - \vec{\nabla}. (\vec{B} \vec{\nabla} \eta) + \vec{\nabla}. (\vec{\nabla} \eta \vec{B}))$$

$$= 0$$

This will allow us to determine the final induction equation in the following manner.

$$\frac{\partial \vec{B}}{\partial t} + \frac{1}{\mu_0} \left(\vec{\nabla} \left(\vec{\nabla}. (\eta \vec{B})\right) - \vec{\nabla}^2 (\eta \vec{B}) - \vec{\nabla}. (\vec{B} \vec{\nabla} \eta) + \vec{\nabla}. (\vec{\nabla} \eta \vec{B})\right)$$

$$+ \vec{\nabla}. (\vec{U} \vec{B}) - \vec{\nabla}. (\vec{B} \vec{U}) = 0;$$

(3.34)

3.3 Summary of the Derived Governing Equations.

Let's represent the deducted final equations (3.27), (3.28), (3.33) and (3.34) to make it clear and easier for a reader to see through the equations and compare with the adopted governing equations which will be presented later on.

The Continuity Equation:

$$\frac{\partial \rho}{\partial t} + \vec{\nabla}.(\rho\vec{u}) = 0$$

The Magneto-hydrodynamics Momentum Equation:

$$\frac{\partial(\rho\vec{U})}{\partial t} + \vec{\nabla}.(\rho\vec{U}\vec{U}) - \vec{U}\left(\frac{\partial \rho}{\partial t} + \vec{\nabla}.(\rho\vec{U})\right)$$

$$= -\vec{\nabla}P + \frac{1}{\mu_0}\vec{\nabla}(\vec{B}.\vec{B}) - \frac{1}{\mu_0}(\vec{\nabla}.\vec{B})\vec{B} - \vec{\nabla}\left(\frac{B^2}{2\mu_0}\right);$$

The Magneto-hydrodynamics Magnetic Induction Equation:

$$\frac{\partial \vec{B}}{\partial t} + \frac{1}{\mu_0}\left(\vec{\nabla}\left(\vec{\nabla}.(\eta\vec{B})\right) - \vec{\nabla}^2(\eta\vec{B}) - \vec{\nabla}.(\vec{B}\vec{\nabla}\eta) + \vec{\nabla}.(\vec{\nabla}\eta\vec{B})\right)$$

$$+ \vec{\nabla}.(\vec{U}\vec{B}) - \vec{\nabla}.(\vec{B}\vec{U}) = 0;$$

The Magneto-hydrodynamics Total Energy Equation:

$$\frac{\partial\left(\rho e+\frac{1}{2}\rho U^{2}+\frac{B^{2}}{2\mu_{0}}\right)}{\partial t}+\vec{\nabla}.\left(\rho\vec{U}e+\frac{1}{2}\rho U^{2}\vec{U}+\vec{U}\left(\frac{B^{2}}{2\mu_{0}}\right)\right)$$

$$-e\left(\frac{\partial\rho}{\partial t}+\vec{\nabla}.\left(\rho\vec{U}\right)\right)-\frac{1}{2}U^{2}\left(\frac{\partial\rho}{\partial t}+\vec{\nabla}.\left(\rho\vec{U}\right)\right)$$

$$+\frac{\vec{\nabla}}{\mu_{0}}.\left(\frac{\eta}{\mu_{0}}\vec{\nabla}\left(\vec{B}.\vec{B}\right)\right)-\frac{\vec{\nabla}}{\mu_{0}}.\left(\frac{\eta}{\mu_{0}}\left(\vec{\nabla}.\vec{B}\right)\vec{B}\right)$$

$$-\frac{\vec{\nabla}}{\mu_{0}}.\vec{\nabla}\left(\eta\frac{B^{2}}{2\mu_{0}}\right)-\frac{\vec{\nabla}}{\mu_{0}}.\left(\vec{B}\left(\vec{U}.\vec{B}\right)\right)$$

$$=-P\vec{\nabla}.\vec{U}-\vec{U}.\vec{\nabla}P-\vec{\nabla}(\frac{B^{2}}{2\mu_{0}}\vec{U});$$

3.4 Adopted Magneto-Hydrodynamics Equations

The Continuity Equation remains unchanged as follows:

$$\frac{\partial\rho}{\partial t}+\vec{\nabla}.\left(\rho\vec{u}\right)=0$$

According to the Gauss' law of magnetism, the divergence of the magnetic field vector is zero which means that there will be an exhibition of a closed loop magnetic system in the domain. Therefore, the momentum equation could be expressed:

$$\frac{\partial\left(\rho\vec{U}\right)}{\partial t}+\vec{\nabla}.\left(\rho\vec{U}\vec{U}\right)-\vec{U}\left(\frac{\partial\rho}{\partial t}+\vec{\nabla}.\left(\rho\vec{U}\right)\right)=-\vec{\nabla}P+$$

$$\frac{1}{\mu_{0}}\vec{\nabla}\left(\vec{B}.\vec{B}\right)-\vec{\nabla}\left(\frac{B^{2}}{2\mu_{0}}\right); \qquad \textbf{(3.35)}$$

In fact, the two last terms are nothing but the Lorentz force activated by the built-in Magneto-hydrodynamics module located in FLUENT as a momentum source term. Regarding the magnetic induction equation, the electrical resistivity is assumed as a uniform parameter in space so that all of the terms of Eq(3.34) could be neglected except the convective, the transient and the magnetic diffusion terms where the latter is thrown in the right hand side to be considered as a magnetic source term as such:

$$\frac{\partial \vec{B}}{\partial t} + \vec{\nabla}.\left(\vec{U}\vec{B}\right) - \vec{\nabla}.\left(\vec{B}\vec{U}\right) = \frac{1}{\mu_0}\vec{\nabla}^2\left(\eta\vec{B}\right); \qquad \textbf{(3.36)}$$

Finally, let's satisfy the divergence free condition as well as the conservation of mass equation where the net mass flow rate is null. On the other hand, it is required to respect ANSYS FLUENT's energy equation written in the theory guide by adding the transient magnetic energy term and the convective energy term into the right hand side as sources terms leading to the following Total Energy equation:

$$\frac{\partial\left(\rho e+\frac{1}{2}\rho U^2\right)}{\partial t} + \vec{\nabla}.\left(\rho\vec{U}e + \frac{1}{2}\rho U^2\vec{U}\right) = -P\vec{\nabla}.\vec{U} - \vec{U}.\vec{\nabla}P -$$

$$\frac{\vec{\nabla}}{\mu_0}.\left(\frac{\eta}{\mu_0}\vec{\nabla}\left(\vec{B}.\vec{B}\right)\right) + \frac{\vec{\nabla}}{\mu_0}.\vec{\nabla}\left(\eta\frac{B^2}{2\mu_0}\right) - \vec{\nabla}.\left(\left(\frac{B^2}{2\mu_0}\right)\right) + \frac{\vec{\nabla}}{\mu_0}.\left(\vec{B}\left(\vec{U}.\vec{B}\right)\right) -$$

$$\vec{\nabla}\left(\frac{B^2}{2\mu_0}\vec{U}\right) - \frac{\partial\left(\frac{B^2}{2\mu_0}\right)}{\partial t} + k_{eff}\nabla T; \qquad \textbf{(3.37)}$$

Where the last term represents the thermal conduction which is located in the built-in energy equation's module of FLUENT and it is written in the ANSYS theory guide.

Therefore, the thermal diffusion term is coupled to the energy equation and automatically computed by the FLUENT algorithm.

3.5 Case Study's Numerical Setup.

Several previous research papers in the literature are probed and analyzed and since the thesis' objectives is dealing with plasma aerodynamics, especially the interaction between hot plasmas' shockwaves and oblique shockwaves generated by the supersonic or hypersonic flows, SUN QUAN's research paper mentioned in the literature review's chapter above is taken in a consideration as a main project to focus on and to make a comparison with its contour plots' results. It is necessary to adopt the mentioned project's geometry, to build it with a high precision using the Design Modeler situated within ANSYS FLUENT and to use the same models, equations and boundary conditions used by SUN QUAN in order to successfully validate the results so that to be able to expand the additional magneto-hydrodynamics equations and parameters which characterizes the lightning discharge and to earn the confidence as well as a kind of credibility of the interaction's desired numerical results. In fact, it is about a 25° ramp problem to deal as mentioned in the targeted article where the compression corner is bounded by the Inlet in the end of the left hand side and by the outlet in the end of the right hand side, in addition to the top is regarded as a free stream air flow with a Mach number of 3. On the other hand, the lightning discharge is modeled by dividing the ambient domain into two zones, the first one is the air domain whereas the second one will be the lightning plasma zone restricted by two open interfaces which allows any flow to diffuse it without causing any cell face blockage to be happened. As implied by SUN QUAN that the compression procedure is done with

the help of shockwaves generated by the ramps without using the compressors where these kinds of inlets are adopted by a few turbojet engines but the majority of the applications of the Inlet self compressions are studied and performed in the area of SCRAMJET and RAMJET engines.

A screenshot taken from ANSYS clarifies the aforementioned description about the Scramjet's Compression Corner Geometry which is shown below:

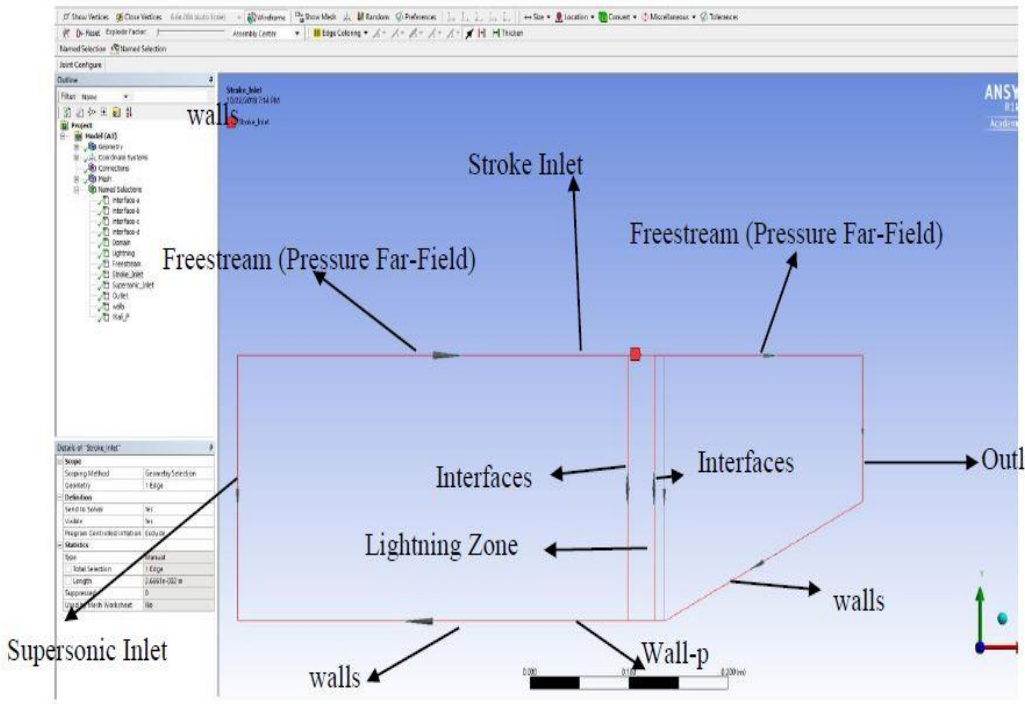

FIG.17. SUN QUAN's Compression Corner built with Design Modeler (Source*: AUB CFD LAB's ANSYS)*

Furthermore, many efforts are made in order to obtain an efficient mesh leading to a better convergence. In fact, this mesh consists of 129692 elements where the structured quadrilateral grids predominate in the computational domain. On the other hand, a projection is designed as y-axis located at the foot of the ramp to make the cells oriented in parallel to the inclined wall which improve the compatibility between the cells, precisely each element face with the velocity vectors which will get inclined with the

ramp while producing the shockwave. So the latter strategy makes it easier to converge and provides logical and more realistic results. Moreover, the inflation layers are used as a final tool to empower the validity of the desired simulation where these layers were helpful to trigger the appearance of the separation bubble between the inclined and the grounded walls. The structure of the mesh is shown below and it is performed by Mesh Modeler, a tool that belongs to ANSYS.

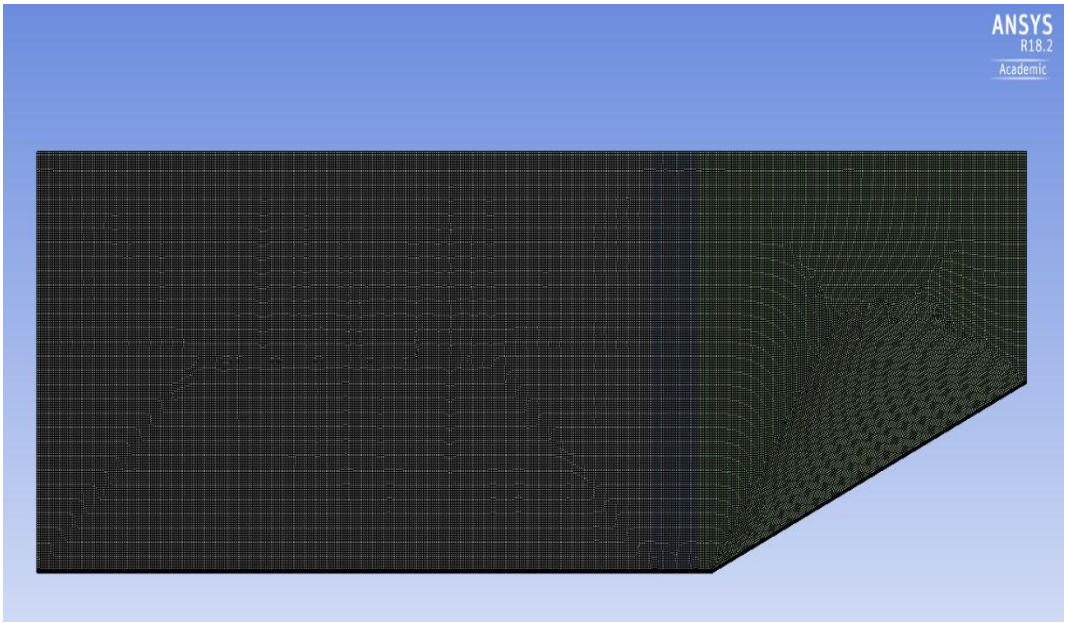

FIG.18. SUN QUAN's Compression Corner's Mesh performed using Mesh Modeler (Source*: AUB CFD LAB's ANSYS)*

The inflation layers responsible for the boundary layer structure improvement as well as the separation layer's existence, will be represented in figure.18 as such:

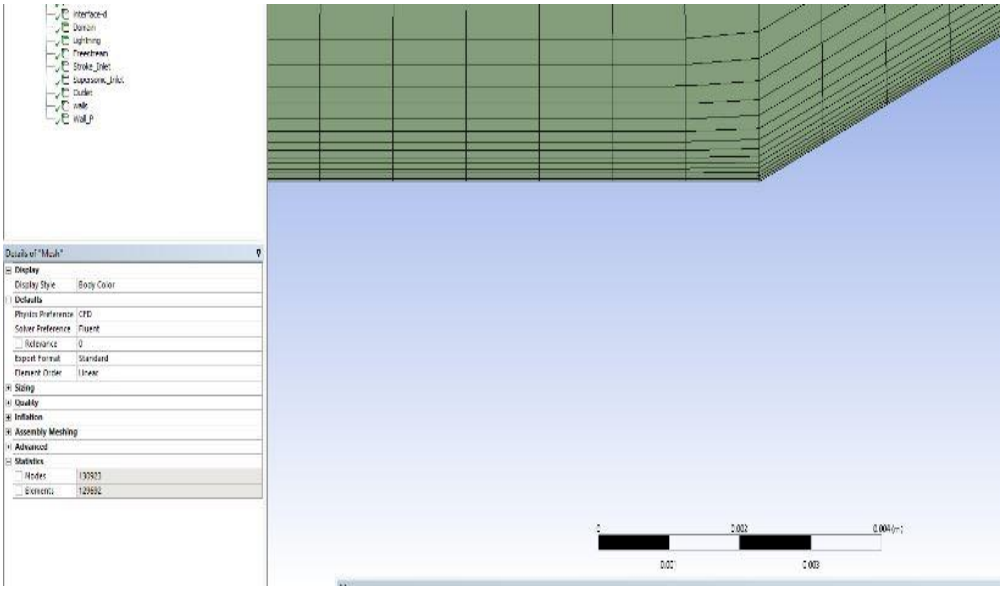

FIG.19. SUN QUAN's Compression Corner's Inflation Layers performed using Mesh Modeler (Source*: AUB CFD LAB's ANSYS)*

After performing the procedure of the mesh, it is required to get into the FLUENT setup where the additional equations could be activated, the material properties could be modified as well as the boundary conditions.

Let's begin with the energy equation which is activated through the FLUENT setup and additional User-Defined Scalar terms could be injected into the energy equation using the User-Defined Functions code using the compiler within FLUENT in order to model the lightning channel striking the ramp where the magnetic convective, the transient and the diffusion terms are added to the original energy equation as mentioned above. On the other hand, it is feasible to couple the magneto-hydrodynamics (MHD) magnetic induction equation to the Navier-Stokes Equations using specific commands stated by the MHD FLUENT guide. In addition to these four equations, the transition-SST turbulence model is activated where SST equations are coupled with transition model equations leading to the increase of the precision regarding the separation flow

problems as well as to the improvement of the case study convergence, specifically when the supersonic oblique shockwaves are subjected to sudden high temperature and pressure values.

SIMPLE scheme is adopted to solve for the Navier-Stokes equations where the Second Order Upwind is used for spatial discretization along with the second order implicit method is chosen for transient formulation.

So to make a brief recapitulation, the simulation of a simple supersonic flow over SUN QUAN's ramp is run in a steady state mode to successfully validate the focused article case study. Then, a transient simulation is to be performed to model the lightning discharge by activating the MHD module, adding the UDS source terms and patching the sudden high temperature of 30000 K, the high pressure in the range of 3 500 000 Pa and the initial magnetic field of 1.2 Tesla. Ten Nano-Seconds are used as a time step size to better capture the shockwaves interaction structure details and in order to avoid any kind of numerical divergence. The future parameter results are saved each 100 time steps and the animation mode is triggered in order to see through the variations which have been made during a time interval of ten milliseconds. The resulted contours will be represented in the "Results and Discussions" chapter and the whole set up description will be clarified in the following way.

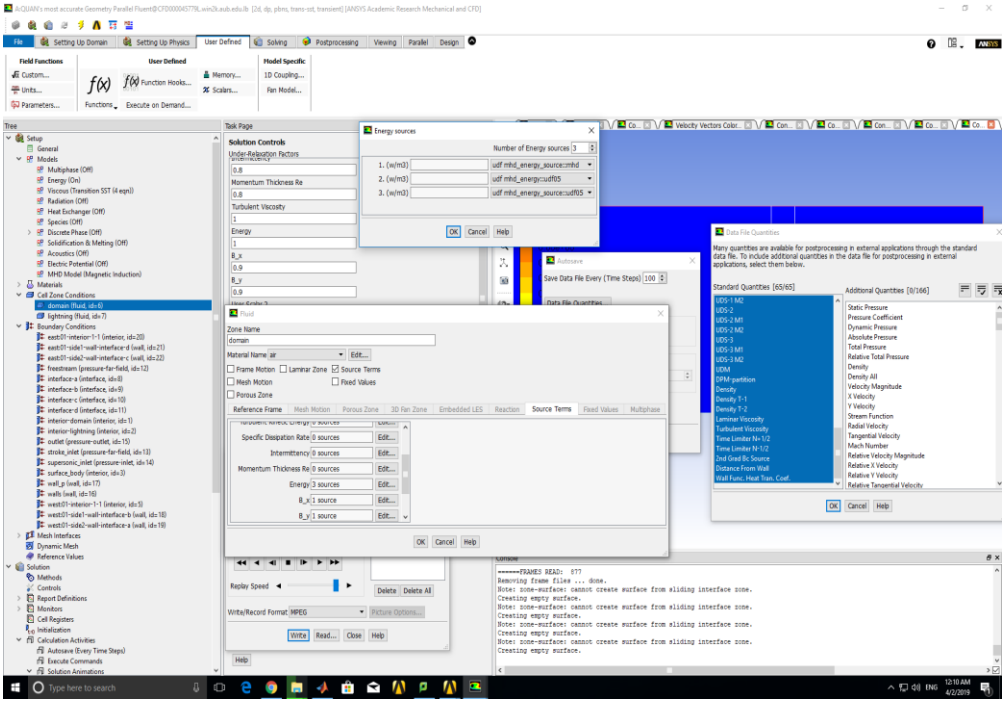

FIG.20. Energy Source Terms added to the ambient air zone of the Lightning-SCRAMJET Inlet's Ramp Case Study (Source*: AUB CFD LAB's ANSYS)*

In Fact, the added energy source terms are shown in the figure above where it is added the ambient air zone called Domain and the same procedure is made in the Lightning zone since the magneto-hydrodynamics equations are solved throughout the whole domains and zones.

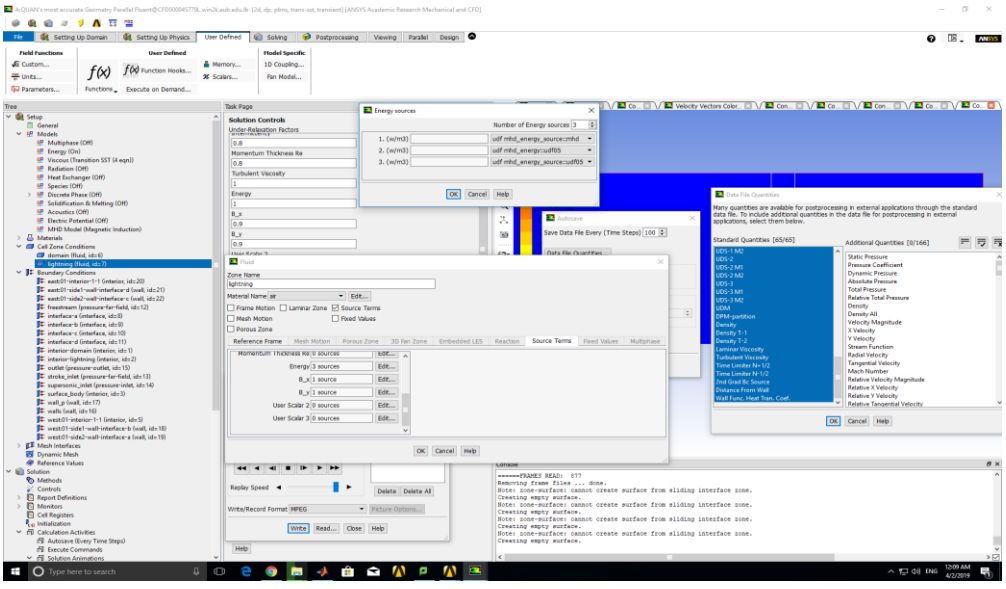

FIG.21. Energy Source Terms added to the lightning zone of the Lightning-SCRAMJET Inlet's Ramp Case Study (Source*: AUB CFD LAB's ANSYS)*

The figure above asserts that the energy source terms related to the magnetic field are added to the lightning zone. In fact, the lightning strike is simulated in a transient state where the sudden high parameters are initially patched in the middle of the lightning zone and then it travels with time along the compression ramp. Therefore, it is imperative to activate the MHD module as well as the added source terms in the ambient air and lightning zones domain in order to discover what will happen to the magnetic field and to visualize its effect on other variables in the whole computational domain.

Figure.22 demonstrates that the magneto-hydrodynamics magnetic induction equation along with its unsteady and convective terms (knowing that the diffusion term of the magnetic induction equation is activated as a source term so that it is taken in the right hand side) are applied in all zones. On the other hand, there exist four user defined scalars where UDS-0 represents the x-component of the magnetic field vector, the UDS-1 is the y-component of the magnetic field vectors whereas UDS-2 and UDS-3 are the scalars that are created to designate respectively the first derivative of UDS-0 and UDS-1 which leads to the computation of the second derivative that is useful to calculate the additional magnetic terms of the energy equation.

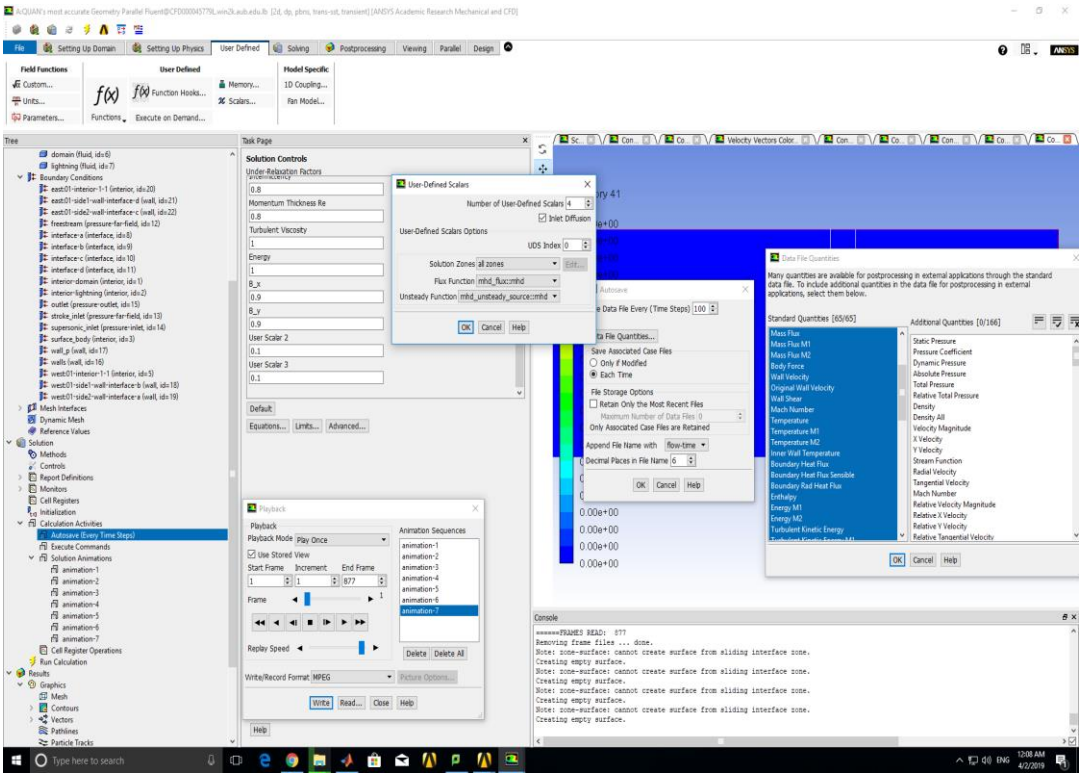

FIG.22. MHD User Defined Scalars (Source*: AUB CFD LAB's ANSYS)*

Fig.23 represents the MHD module where the induction equation could be numerically initialized. Furthermore, the Lorentz force and the Joule effect could be activated using this module window. As we can see the under-relaxation factors given for the magnetic fields components are 0.9 and those provided to the first derivatives of Bx and By are 0.1 for a better convergence.

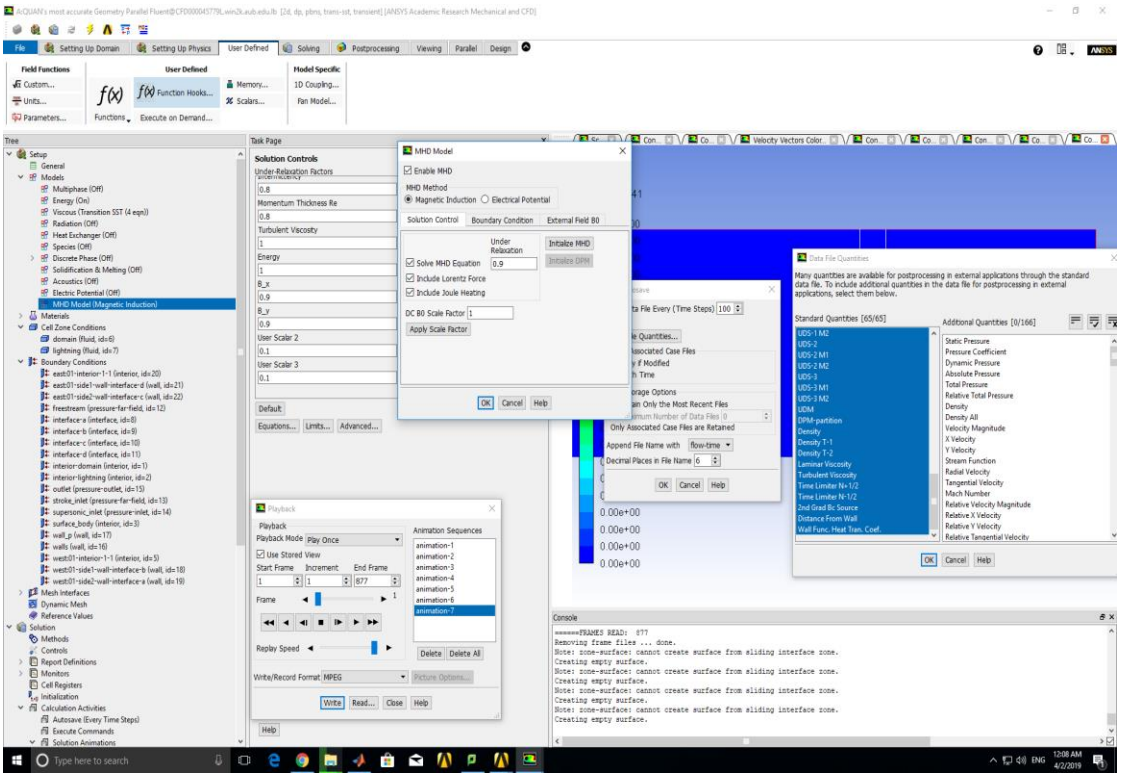

FIG.23. MHD module's window (Source*: AUB CFD LAB's ANSYS)*

Finally, let's discuss about the boundary conditions where it is applied in a similar way before the after the lightning strike. The following parameters and variable values are implied and deduced from SUN QUAN's research paper.

In fact, the Supersonic Inlet as described in Fig.16, is characterized as a Pressure Inlet where the Supersonic/Initial Gauge Pressure is 101325 Pa (1 atmosphere) leading to a gauge total pressure of 3721943 provided that the incoming airflow is at a Mach number of 3, the static temperature is given as 300 K.

The Outlet is treated as a Pressure Outlet where the Gauge Pressure value is also for one Atmosphere.

The type Stroke Inlet and Free-stream boundary conditions is the Pressure Far-Field where the Mach Number of the incoming flow is specified as 3 and the Gauge Pressure is also for 1 atmosphere as performed in the article to be compared.

The Value of the computed Total Temperature is 840 K.

The following figure represents the boundary conditions used for the steady simulation where there is no lightning as well as for the transient mode performed while the intense thunderbolt strikes the compression corner.

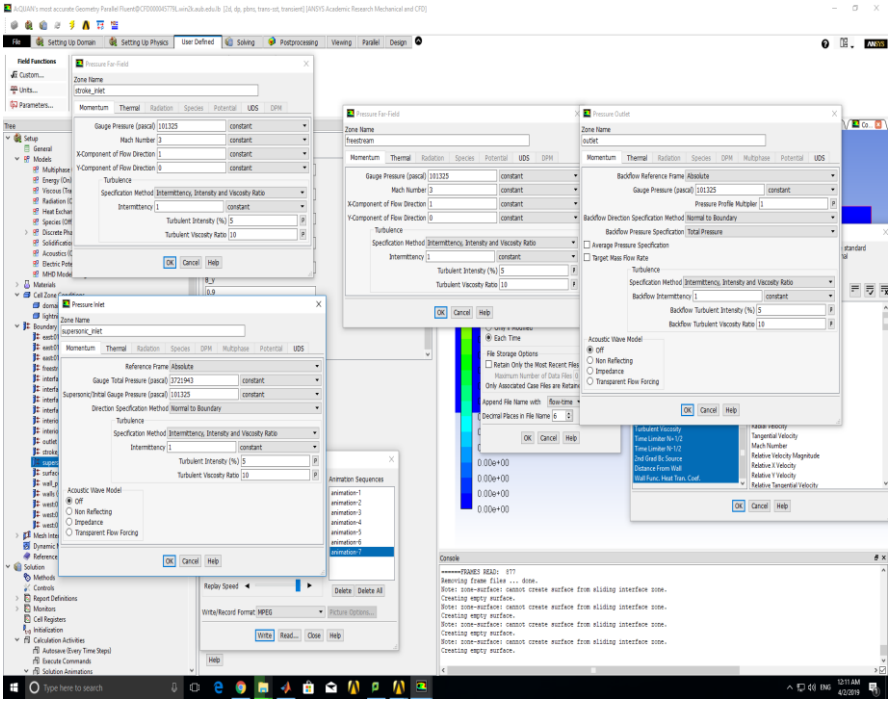

FIG.24. Lightning-SCRAMJET Inlet's Ramp Case Study's Boundary Conditions (Source*: AUB CFD LAB's ANSYS*)

A second case study validation is made where a rectangular plasma MEMS actuator is placed 10 mm apart from the foot of the ramp. As a matter of fact, SUN QUAN regards the plasma actuator as a thermal source term where he attached a constant value into the right hand side of the plasma zone's energy equation. In this thesis, simulations are made to validate SUN QUAN's contour plots in order to make additional approximations where the plasma MEMS actuator's spark discharge could be treated as a magneto-hydrodynamics space plasma device where the full MHD equations are added into the plasma zone along with the constant value energy source term and the results will be shown in the following chapter.

CHAPTER 4

RESULTS AND DISCUSSIONS.

First of all, The Baseline of the desired article is validated in a successful way where the energy equation is activated as well as for the transition SST four equations. Initially the simulation of the baseline is run in a steady state without using the magneto-hydrodynamics equations and without patching the sudden high variables. As a matter of fact, the transition SST turbulence model is adopted in order to increase the convergence with respect to the RSM which leads to undesirable results with a deficient convergence.

The separation bubble is better shown using the transition SST model where the former is an essential phenomenon to probe for the hypersonic aircraft purposes. On the other hand, the separation bubble is an important observable event to investigate in the field of plasma aerodynamics where the plasma can affect the size of the bubble as well as its structure and parameters. It is required to attach the research paper and the thesis' baselines on top of each other through contour plots screenshots to make a proof of their similarities where it makes the succeeding results more trustful and credible. The following two figures represent the Static Pressure Contours of SUN QUAN's baseline on the top whereas the current thesis validation on the bottom.

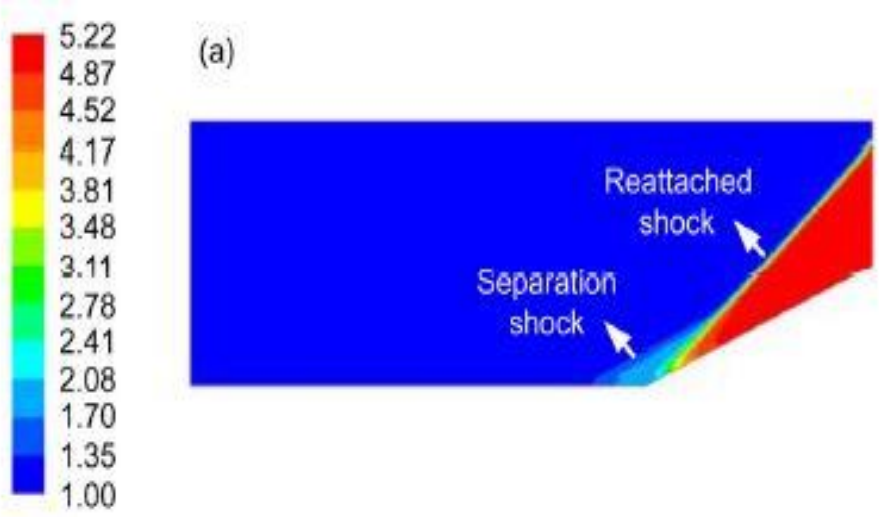

Fig.25. SUN QUAN's Baseline Static Pressure Contour (Source: SUN Quan, LI YingHong, CUI Wei, CHENG BangQin, LI Jun & DAI Hui, "Shock wave-boundary layer interactions control by plasma aerodynamic actuation",Science and Technology on Plasma Dynamics Laboratory,SCIENCE CHINA ,(China, May 2014))

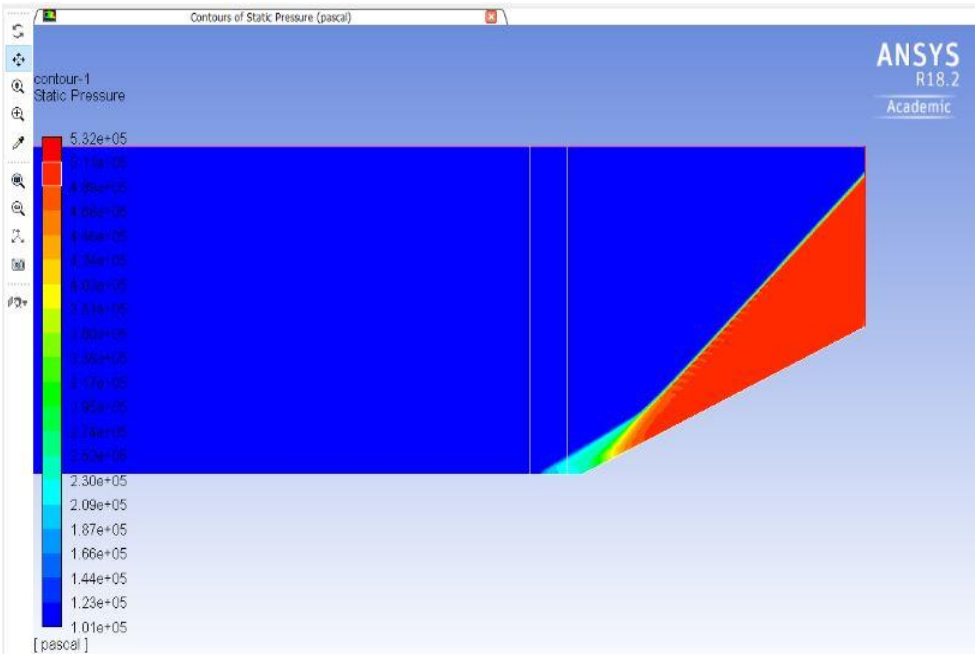

FIG.26. Thesis' Baseline Validation Static Pressure Contour (Source*: AUB CFD LAB's ANSYS)*

Moreover, the validated baseline's temperature plot asserts the similarity of SUN QUAN's contour as such:

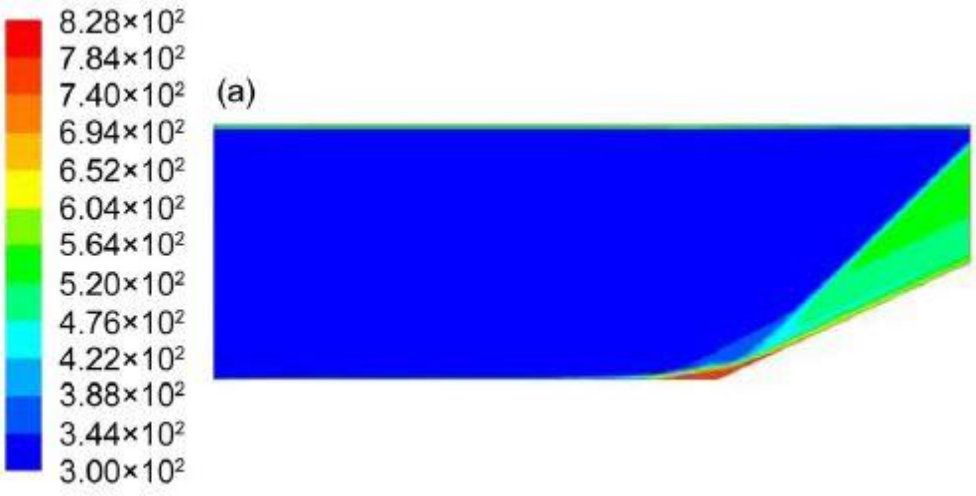

Fig.27. SUN QUAN's Baseline Static Temperature Contour (Source: SUN Quan, LI YingHong, CUI Wei, CHENG BangQin, LI Jun & DAI Hui, "Shock wave-boundary layer interactions control by plasma aerodynamic actuation",Science and Technology on Plasma Dynamics Laboratory,SCIENCE CHINA ,(China, May 2014))

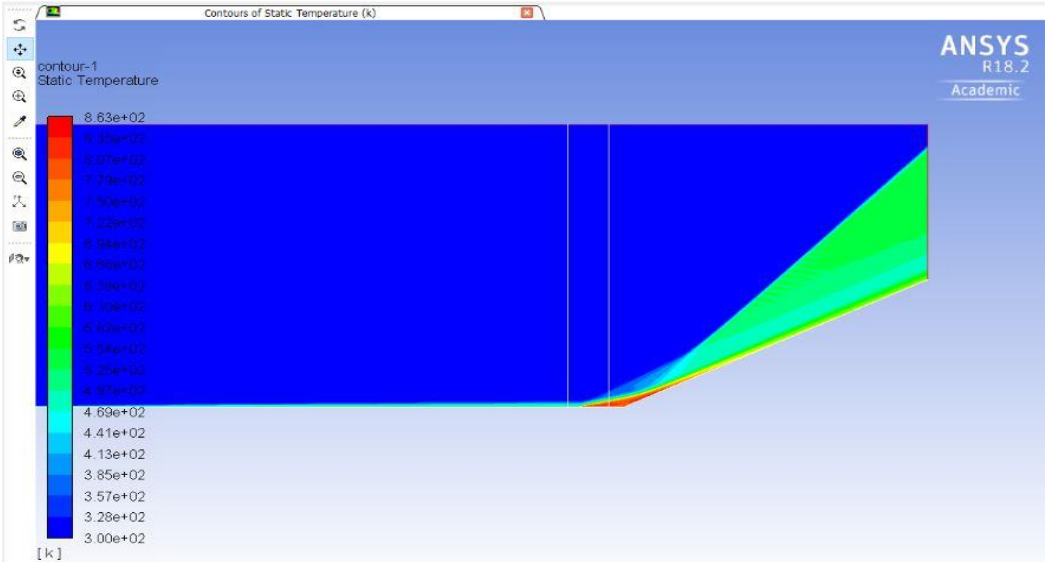

FIG.28. Thesis' Baseline Validation's Static Temperature Contour (Source*: AUB CFD LAB's ANSYS)*

When the steady state is reached (Baseline Validation), transient simulations are performed in order to model the propagating lightning spark throughout the ramp. The Lightning-Scramjet's compressor corner interaction is simulated in two approximations. The first approximation is when the MHD equations are taken into consideration without adding the pointing flux terms as well as the transient magnetic energy term, whereas the second approximation is when it comes to numerically compute the additional magnetic source terms as shown in Eq.(3.37) :

$$\frac{\partial\left(\rho e+\frac{1}{2}\rho U^{2}\right)}{\partial t}+\vec{\nabla}.\left(\rho\vec{U}e+\frac{1}{2}\rho U^{2}\vec{U}\right)$$

$$=-P\vec{\nabla}.\vec{U}-\vec{U}.\vec{\nabla}P-\frac{\vec{\nabla}}{\mu_0}.\left(\frac{\eta}{\mu_0}\vec{\nabla}(\vec{B}.\vec{B})\right)$$

$$+\frac{\vec{\nabla}}{\mu_0}.\vec{\nabla}\left(\eta\frac{B^{2}}{2\mu_0}\right)-\vec{\nabla}.\left(\left(\frac{B^{2}}{2\mu_0}\right)\right)+\frac{\vec{\nabla}}{\mu_0}.\left(\vec{B}(\vec{U}.\vec{B})\right)$$

$$-\vec{\nabla}\left(\frac{B^{2}}{2\mu_0}\vec{U}\right)-\frac{\partial\left(\frac{B^{2}}{2\mu_0}\right)}{\partial t}+k_{eff}\nabla T;$$

The following figures will represent what will happen when the lightning strikes the steady state (Baseline) supersonic flow over a Scramjet's ramp at four time steps. The top figure demonstrates the first approximation where the magneto-hydrodynamics module is activated without any additional terms and the bottom figure reveals the results of the second approximation where the full energy equation(3.37) is taken into account.

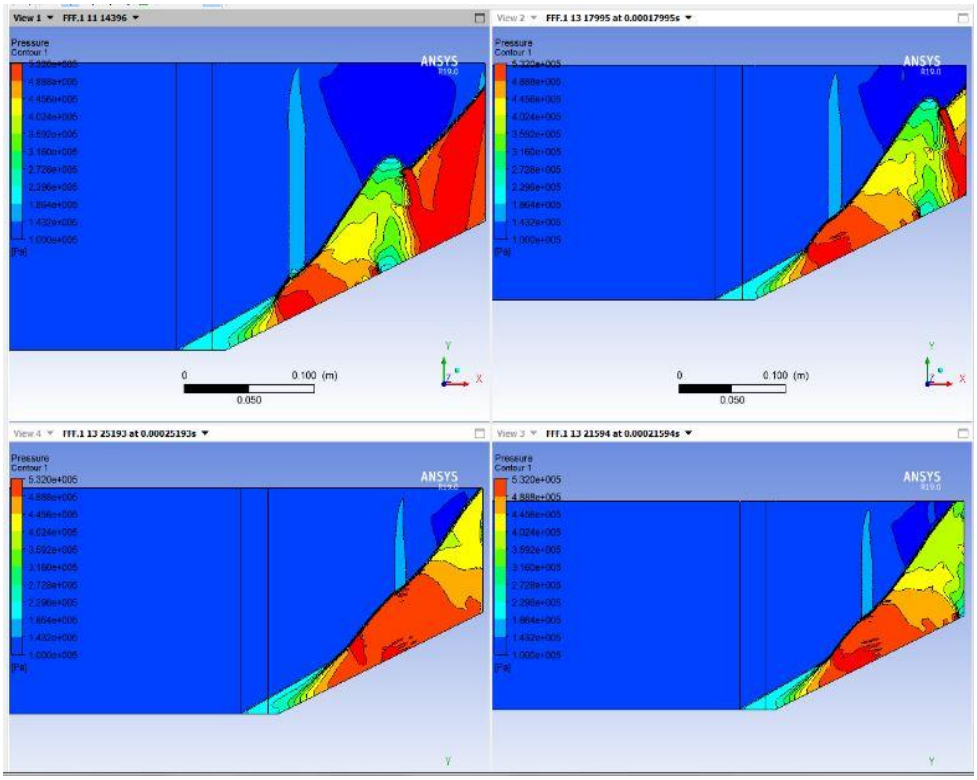

FIG.29. Lightning Scramjet's Ramp Interaction Static Pressure 1st Approximation (Source*: AUB CFD LAB's ANSYS)*

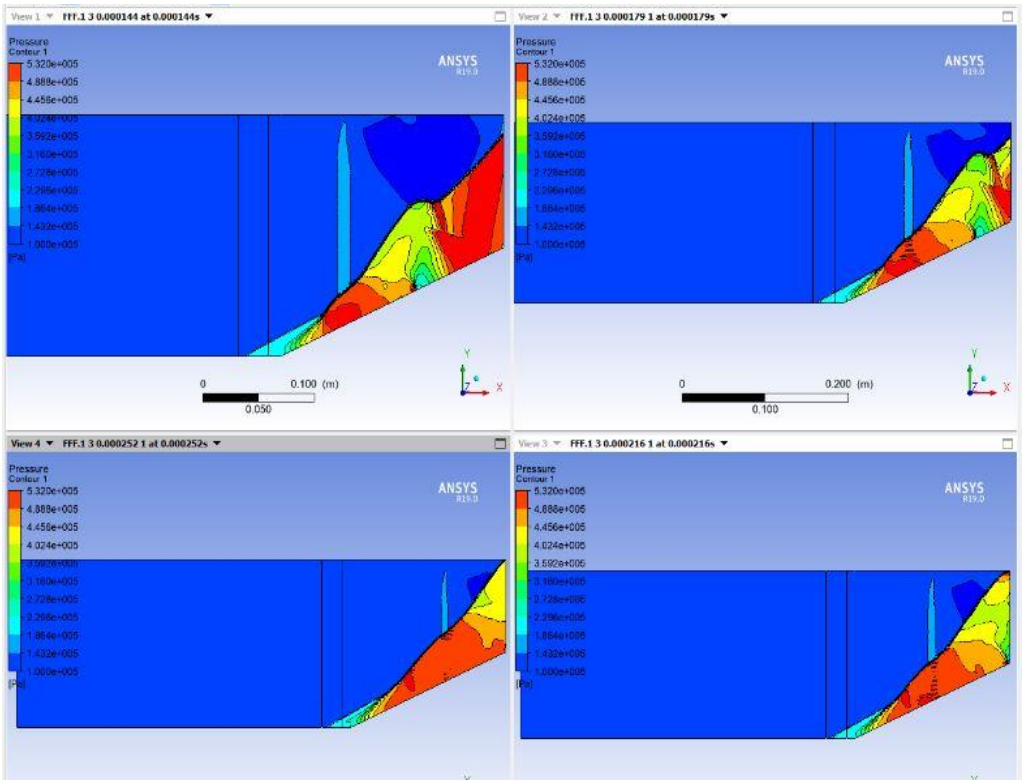

FIG.30. Lightning Scramjet's Ramp Interaction Static Pressure 2nd Approximation (Source*: AUB CFD LAB's ANSYS)*

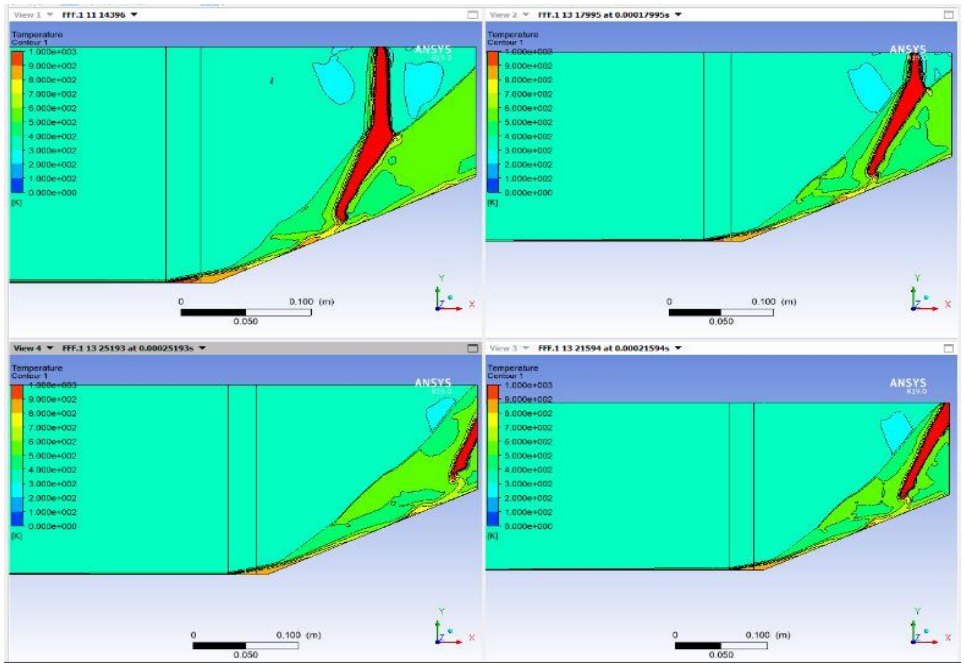

FIG.31. Lightning Scramjet's Ramp Interaction Static Temperature 1st Approximation (Source*: AUB CFD LAB's ANSYS)*

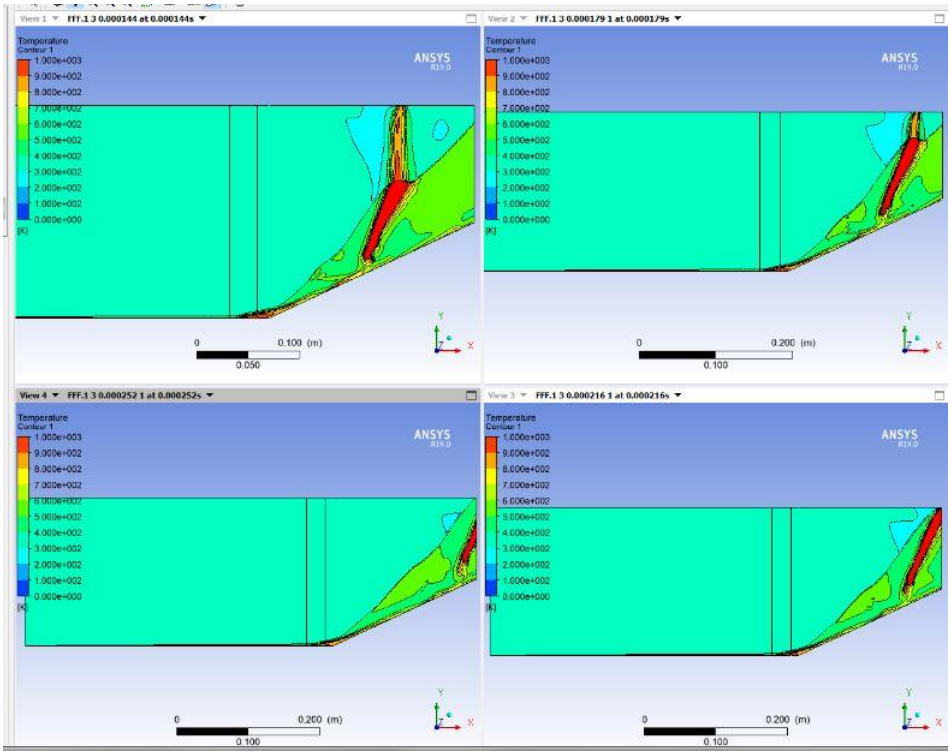

FIG.32. Lightning Scramjet's Ramp Interaction Static Temperature 2nd Approximation (Source*: AUB CFD LAB's ANSYS)*

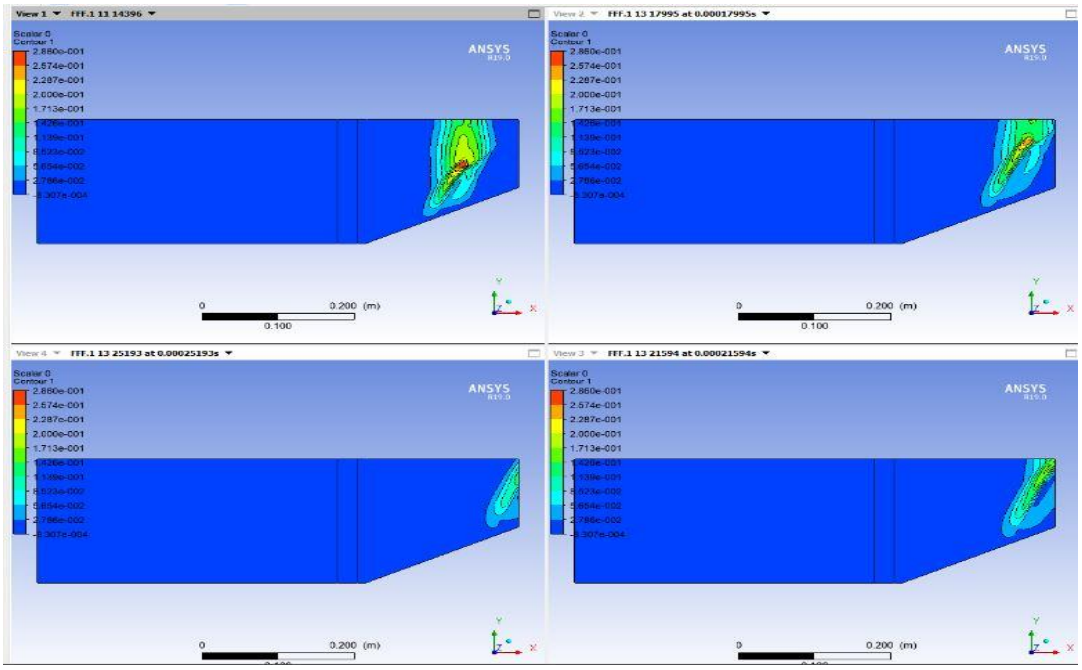

FIG.33. Lightning Scramjet's Ramp Interaction, Magnetic Field's X-Component 1st Approximation (Source*: AUB CFD LAB's ANSYS)*

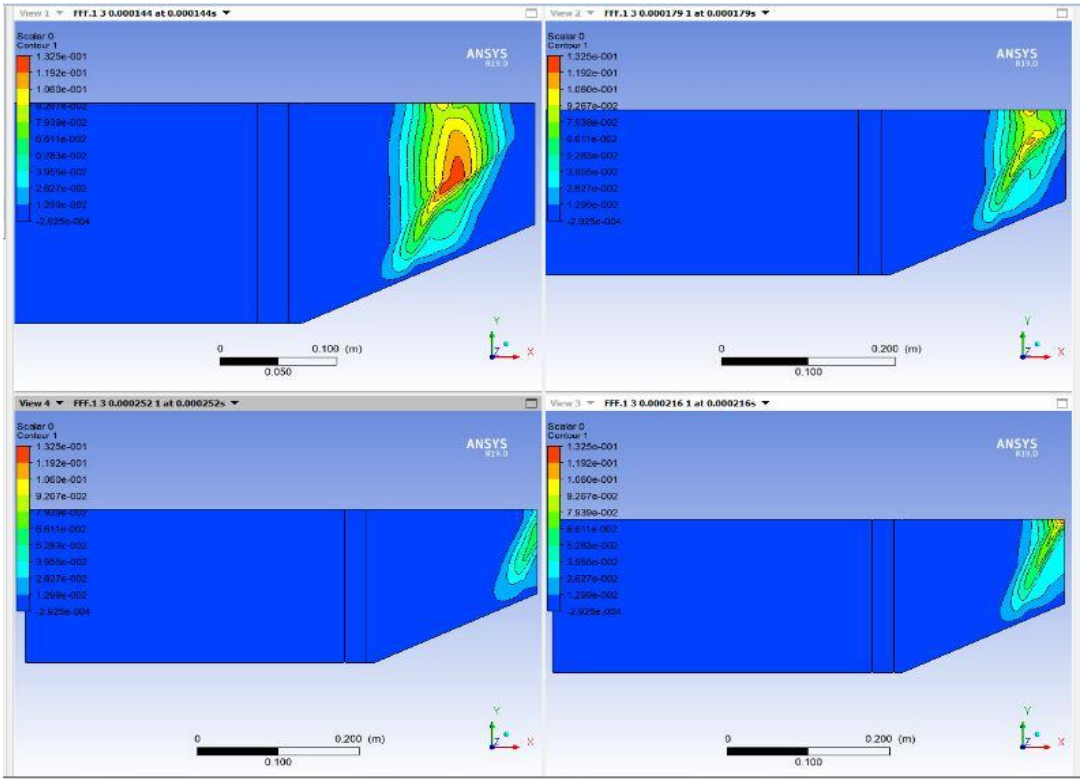

FIG.34. Lightning Scramjet's Ramp Interaction, Magnetic Field's X-Component 2nd Approximation (Source*: AUB CFD LAB's ANSYS)*

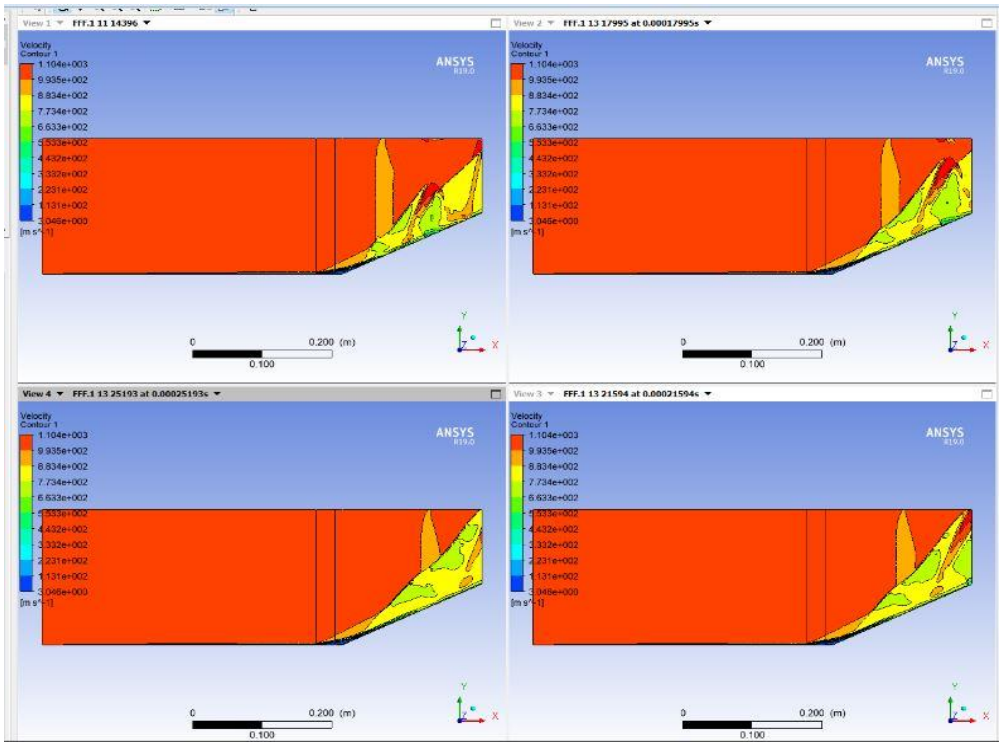

FIG.35. Lightning Scramjet's Ramp Interaction, Velocity Magnitude 1st Approximation (Source*: AUB CFD LAB's ANSYS)*

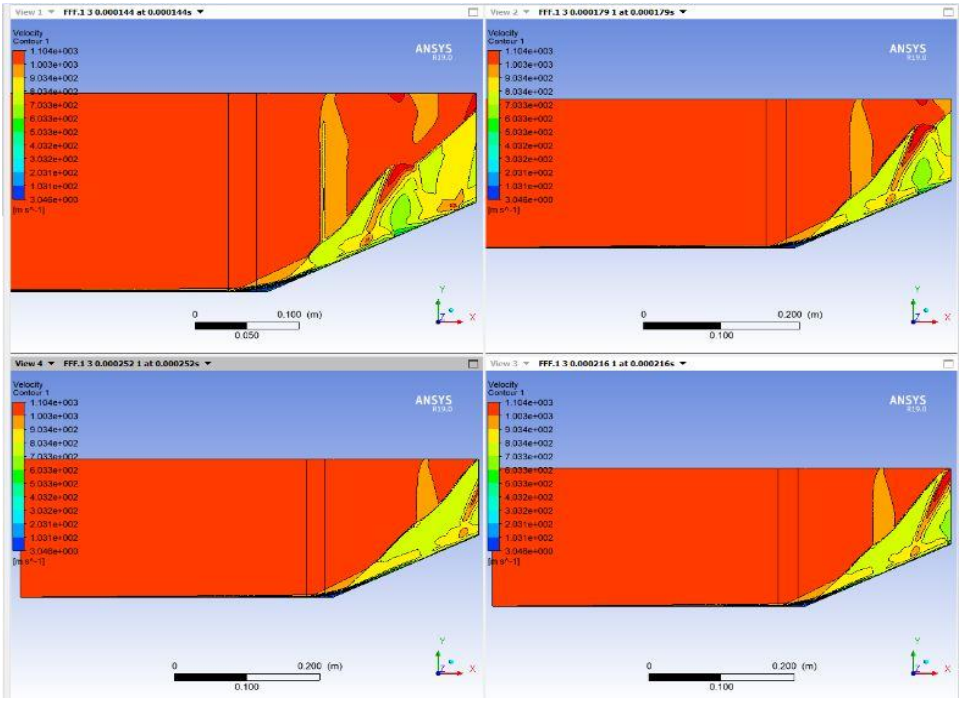

FIG.36. Lightning Scramjet's Ramp Interaction, Velocity Magnitude 2nd Approximation (Source*: AUB CFD LAB's ANSYS)*

Let’s begin with the general analysis which covers the two aforementioned approximations. It is concluded from the pressure, temperature and velocity contours that the oblique shockwave due to the supersonic flow over the ramp get curved. According to Qianhong Zhou’s research paper[24], the shockwave characterized by a high velocity and subjected or located in an extremely hot temperature axial region get curved throughout the compression corner in a simultaneous way with the passage of the lightning strike along the ramp.

As we can see from the pressure contours that the separation shockwaves get lifted and elongated in order to seek for an end point to intercept with, which leads to the separation bubble enlargement.

Another theory which is able to explain the result that is in the process of investigation. Based on the shockwave boundary layer interaction’s theory, when the boundary layer is subjected to an adverse strong pressure gradient issued from an incident shockwave, provided that the boundary layer cannot support the incoming pressure, it separates to create a separation bubble where the neighboring compression waves coalesce to form the separation oblique shockwave. In our case, the adverse pressure gradient surrounding the separation bubble is intensified by the lightning strike cylindrical shockwave to lead to a further deflection of the separation bubble. On the other hand, the high temperature along with the high pressure effects which is travelling through the whole oblique shockwave structure causes the coalesced compression waves to move backward leading to the separation shock expansion.

Moreover, at the instantaneous time period 0.00014396 the resultant of the interaction between the separation and the reattachment shockwaves collides with the propagating cylindrical shockwave generated by the powerful thunderbolt leading to a mach stem[25]

formation. As long as the lightning discharge is traveling along the ramp, the mach stem will be elongated until it will be vanished when the cylindrical shockwave will be totally escaped from the outlet so that the oblique structure returns to its original steady state. This deduced phenomenon is better represented in the velocity contour plots (Fig.34 and Fig.35).

Furthermore, as it is deduced from the temperature contours (Fig.30 and Fig.31), the lightning bolt bombards the oblique shockwave which will be deflected in a clockwise way downstream the shock creating a weaker static pressure nearby as described in Fig.28 and Fig.29.

Regarding the magnetic field in both approximations, the magnetic field lines which form a closed loop along the compression corner get deflected while crossing the oblique shockwave. The reason of the field lines' sudden change is because of the coupling between the magnetic field and the velocity field, knowing that the velocity vectors change their orientation just after the oblique shockwave. On the other hand, the closed loop of the magnetic field lines in the second approach becomes more diffused, which means the field lines will be spread out leading to a loop area enlargement. This dilatation is due to the term representing the flux of the Lorentz force where its derivation leads to the second derivative of the magnetic field which is nothing but the diffusion term of the magnetic field.

In fact, the magnetic field resulted from the first approach where it is computed using the built-in magneto-hydrodynamics equations has a maximum value of 0.2860 Tesla whereas the magnetic peak value will be decreased to 0.1325 Tesla. Obviously, this effect comes into existence due to the injection of the additional terms such as the magnetic energy transient term, the magnetic convective term as well as the

magnetic diffusion term or the flow of the Lorentz force added to the energy equation. It could be analyzed that the magnetic energy convective and diffusion terms expand the enclosed magnetic field lines so that the magnetic field and forces exerted by the moving charged particles will be diffracted throughout a larger area or in other words the magnetic field will be advected and diffused in a longer range unlike in the first approach where the magnetic field energy has no diffusion and convection terms which makes the magnetic field loop more restricted to lead to a higher magnetic intensity than that of the 2^{nd} approach knowing that the same initial conditions and parameters are used for the two approximations.

CHAPTER 5

CONCLUSION AND RECOMMENDATIONS.

The simulation of a supersonic flow travelling with a speed of Mach 3 over a compression ramp is made and compared with the SUN QUAN's baseline. In fact, the focused plots which are to be compared are successfully validated in order to model the thunderbolt interacting the ramp flowing in a supersonic flow and to make the resulted contour plots more trustful and credible. In the current thesis, the lightning discharge is modeled using the macroscopic approach where the FLUENT built-in magneto-hydrodynamics are used for the first approximation whereas the magnetic energy convective, transient and diffusion terms are added to the energy equation to produce the full adopted magneto-hydrodynamics capable to simulate the lightning discharge in a more realistic way and regarded as a second approximation.

The most important features acquired from the whole thesis' post processing results are summarized below as such:

The separation and reattachment shockwaves are elongated due to their interaction with the cylindrical shockwave produced by the lightning.

The oblique shockwave initially produced by the ramp is broken down into two pieces separated by a curved shockwave and this is due to the effect of the sudden axial high temperature generated by the long spark discharge.

The magnetic field closed loops get curved downstream of the oblique shockwave in both approximations.

When the magnetic energy terms are added, the magnetic field closed loop area gets enlarged, as we can see that the peak magnetic value will be decreased with respect to the first approximation's maximum magnetic field.

The separation bubble gets fluctuated and enlarged while the lightning discharge strike the ramp from the corner until the electric spark reaches the outlet.

As a matter of fact, these perturbations are occurred along the compression corner and reach the baseline steady state at a time period of nearly 10 ms.

The purpose of the current work is to fill in the gap of the literature where the aerodynamics effects of the interaction between the lightning discharge and a ramp flowing in a supersonic speed are not studied yet. Moreover, the predicted results are regarded as significant contributions for the full scramjet intake design flowing in the presence of a lightning strike in order to see whether the engine's efficiency will be decreased or it will maintain its level. The full scramjet intake design will be taken into consideration and will be performed as an additional research paper.

The aforementioned theoretical background in the second chapter will be validated using FLUENT numerical code where analytical formulae describing the propagation of a cylindrical strong shockwave in a compressed medium have to be numerically compared, so this will be accomplished as a third research paper.

BIBLIOGRAPHY.

[1] Karol Aniserowicz," Nature of Atmospheric Discharges,"TELEKOMUNIKACJA I TECHNIKI INFORMACYJN,(Feb 2013).

[2] Bert Tayara.,Report, The Netherlands at the Faculty of Aerospace Engineeringof the Delft University of Technology in the Netherlands, Delft, December 2008.

[3] Thomas Neuenhahn," Investigation of the shock wave/boundary layer interaction of scramjet intake flows," Deutsche Nationalbibliothek, RWTH Aachen University, 2010)

[4] Sun, Q., Li, Y., Cui, W., Cheng, B., Li, J., & Dai, H. (2014). Shock wave-boundary layer interactions control by plasma aerodynamic actuation. Science China Technological Sciences, 57(7), 1335-1341. doi:10.1007/s11431-014-5586-1

[5] shao-Chi Lin,"Cylindrical Shock Waves Produced by Instantaneous Energy Release", Journal of Applied Physics, Volume 25, Number 1, (January, 1954).

[6] Geoffrey Taylor, "The Formation of a Blast Wave by a Very Intense Explosion.I. Theoretical Discussion," Proceedings of the Royal Society of London. Series A, Mathematical and Physical Sciences, Vol.201, No. 1065. (Mar. 22, 1950), pp. 159-174.

[7] Chen, Q., Chen, B., Chen, P. F., Xiong, R., & Cai, Z. (2014). A unified radiative magnetohydrodynamics code for lightning-like discharge simulations. Physics of Plasmas, 21(3) doi:10.1063/1.4867663

[8] Wright, D., Delmont, P., & Torrilhon, M. (2013). Modeling of electric arcs: A study of the non-convective case with strong coupling. Journal of Plasma Physics, 79(5), 699-713. doi:10.1017/S0022377813000317

[9] D'Angola, A., Colonna, G., Gorse, C., & Capitelli, M. (2008). Thermodynamic and transport properties in equilibrium air plasmas in a wide pressure and temperature range. European Physical Journal D, 46(1), 129-150. doi:10.1140/epjd/e2007-00305-4

[10] Durna, A. S., Ali Barada, M. E. H., & Celik, B. (2016). Shock interaction mechanisms on a double wedge at mach 7. Physics of Fluids, 28(9) doi:10.1063/1.4961571

[11] Lu, H., Yue, L., Xiao, Y., & Zhang, X. (2013). Interaction of isentropic compression waves with a bow shock. AIAA Journal, 51(10), 2474-2484. doi:10.2514/1.J052373

[12] Luis F. Gutiérrez Marcantoni, José P. Tamagno and Sergio A. Elaskar . "HIGH SPEED FLOW SIMULATION USING OPENFOAM".Mecánica Computacional Vol XXXI, págs. 2939-2959, Salta, Argentina, 13-16 Noviembre 2012.

[13] Kurganov A. and Tadmor E. New high-resolution central schemes for nonlinear conservation laws and convection – diffusion equations. Journal of Computational Physics, 160(1):241 –282, 2000.

[14] C. Fureby, M. Chapuis, E. Fedina & J. Tegnér. "A COMPUTATIONAL STUDY OF SCRAMJET COMBUSTION".Defense Security Systems Technology, The Swedish Defense Research Agency – FOI,Stockholm, Sweden, 2010.

[15] Bensow R. & Fureby C., 2006, "On the Justification and Extension of Mixed Models in LES", J Turbulence 8, p N54.

[16] Baudoin E., Nogenmyr K.J., Bai X.S. & Fureby C.;2009, "Comparison of LES Models applied to a Bluff Body Stabilized Flame", AIAA 2009-1178.

[17] YUFENG YAO and DANIEL RINCON, "SHOCK INDUCED SEPARATING FLOWS IN SCRAMJET INTAKES", International Journal of Modern Physics: Conference SeriesVol. 19 (2012) 73–82.

[18] W. Schuyler Hinman, Craig T. Johansen, Chris J. Arisman, Wagner C. Galuppo "Numerical Investigation of Laminar Near Wake Seperation On Circular Cylinders at Supersonic Velocities", 29th Congress of the International Council of the Aeronautical Sciences. St. Petersburg, Russia, September 7-12, 2014.

[19] Lt Col Troy C. Hoeger, Dr. Paul I. King, and Lt Col Douglas D. Decker ."CFD Modeling of an Isolator Shock Train in a Scramjet Engine"46th AIAA/ASME/SAE/ASEE Joint Propulsion Conference & Exhibition. 2010.

[20] Sudharsan, N.M, Jambekhar, V.A and Babu V. "A validation study of OpenFOAM using the supersonic flow in a mixed compression intake" Proceedings of the Institution of Mechanical Engineers Part G Journal of Aerospace Engineering (Impact Factor: 0.68). 06/2010; 224(6):673-679.

[21] Ramesha D.K., Rudra Murthy, Hemanth Kumar.P , " CFD Analysis of Supersonic Exhaust in a Scramjet Engine", International Journal of Innovative Research in Science,Engineering and Technology (An ISO 3297: 2007 Certified Organization)Vol. 2, Issue 9, September 2013.

[22] Karri Simachalam Naidu and Dinesh Kumar Bajaj. " Modeling and Exhaust Nozzle Flow Simulations in a Scramjet ". International Journal of Science and Research (IJSR) 2013

[23] ANDERSON John , Fundamentals of Aerodynamics , Fourth Edition(International) , McGraw Hill , New York , USA (2007)

[24] Zhou, Q., Dong, Z., & Yang, W. (2016). Revisiting the thermal effect on shock wave propagation in weakly ionized plasmas. Physics of Plasmas, 23(7) doi:10.1063/1.4958640

[25] XIANG, G., WANG, C., TENG, H., & JIANG, Z. (2018). Shock/shock interactions between bodies and wings. Chinese Journal of Aeronautics, 31(2), 255-261. doi:10.1016/j.cja.2017.11.012